AD_____

Award Number: W81XWH-10-1-0105

TITLE: Targeting PCNA Phosphorylation in Breast Cancer

PRINCIPAL INVESTIGATOR: Vincent Jo Davisson, Ph.D.

CONTRACTING ORGANIZATION: Purdue University
West Lafayette, IN 47907

REPORT DATE: April 2013

TYPE OF REPORT: Final

PREPARED FOR: U.S. Army Medical Research and Materiel Command
Fort Detrick, Maryland 21702-5012

REPORT DOCUMENTATION PAGE

Form Approved
OMB No. 0704-0188

1. REPORT DATE	2. REPORT TYPE	3. DATES COVERED
April 2013	Final	15 March 2010 – 14 March 2013

4. TITLE AND SUBTITLE

Targeting PCNA Phosphorylation in Breast Cancer

5a. CONTRACT NUMBER

5b. GRANT NUMBER
W81XWH-10-1-0105

5c. PROGRAM ELEMENT NUMBER

6. AUTHOR(S)

V. Jo Davisson, Anthony Pedley, Qingshou Chen, Matthew Bartolowits
Raymond Fatig

E-Mail: davisson@purdue.edu

5d. PROJECT NUMBER

5e. TASK NUMBER

5f. WORK UNIT NUMBER

7. PERFORMING ORGANIZATION NAME(S) AND ADDRESS(ES)

Purdue University
West Lafayette, IN 47907

8. PERFORMING ORGANIZATION REPORT NUMBER

9. SPONSORING / MONITORING AGENCY NAME(S) AND ADDRESS(ES)
U.S. Army Medical Research and Materiel Command
Fort Detrick, Maryland 21702-5012

10. SPONSOR/MONITOR'S ACRONYM(S)

11. SPONSOR/MONITOR'S REPORT NUMBER(S)

12. DISTRIBUTION / AVAILABILITY STATEMENT
Approved for Public Release; Distribution Unlimited

13. SUPPLEMENTARY NOTES

14. ABSTRACT
PCNA, an essential protein in the DNA synthesis and repair, was shown to be phosphorylated at Y211 by a nuclear kinase. A consequence of this post-translational modification has been highly correlated with a reduced survival rate of breast cancer patients. However, no basic or clinical studies have addressed if these inhibitors down-regulate the nuclear function of the protein. The original observations indicated the EGFR was a major kinase involved in this phosphorylation. Inhibitors of EGFR have exciting potential in treatment but have failed to show clinical efficacy as a mono-therapy treatment option for breast cancer patients. By screening a panel of protein kinase inhibitors in triple negative breast cells for impact on phosphorylation, a direct correlation with EGFR inhibition is not indicated, rather a broader network connecting PCNA modification on chromatin with DNA damage response is implicated. Novel bioconjugates of gefitinib (Iressa) with nuclear targeting peptide-peptoid hybrid sequences have been shown to retain growth inhibitory activity in this context and open avenues for utility in research and new therapies. A new analytical method for enhanced detection of the phosphorylated PCNA isoforms has been shown to be feasible. In addition, by adopting this assay to screen nuclear proteomes of breast tumor cells indicates a more diverse array of PCNA isoforms bearing post-translational modifications opening the door to select specific markers to stage breast cancer patients for molecular therapeutics.

15. SUBJECT TERMS
PCNA, surface enhanced Raman, nuclear localization, kinase pathway inhibitors, DNA replication, DNA repair

16. SECURITY CLASSIFICATION OF:			17. LIMITATION OF ABSTRACT	18. NUMBER OF PAGES	19a. NAME OF RESPONSIBLE PERSON
a. REPORT	b. ABSTRACT	c. THIS PAGE			USAMRMC
U	U	U	UU	45	19b. TELEPHONE NUMBER *(include area code)*

Table of Contents **Page**

Introduction*:* Receptor tyrosine kinases are pivotal players in the control of cellular progression and differentiation. These enzymes predominantly reside at the plasma membrane and initiate signaling cascades as a result of an external stimuli. The expression and dysregulation of ErbB, Eph, and VEGF receptor tyrosine kinases have shown to be present in breast cancer. Recent evidence implicates receptor tyrosine kinases also playing vital roles in downstream processes including tyrosine phosphorylation of non-signaling proteins. Specifically, PCNA, an essential protein in the DNA replication and repair pathways, was previously shown to be phosphorylated at Y211 by a nuclear form of EGFR. A consequence of this alteration has been highly correlated with a reduced survival rate of breast cancer patients. However, no basic or clinical studies have addressed if these inhibitors down-regulate the nuclear function of this protein. Inhibitors of EGFR have exciting potential in other cancer diseases but have failed to show clinical efficacy as a mono-therapy treatment option for breast cancer patients. In addition, therapy resistance in breast cancer patients who initially responded to the inhibitor of ErbB2 receptor tyrosine kinase lapatinib and Iressa are known. Together, these observations call for more specific markers to stage breast cancer patients for effective use of this class of molecular therapeutics.

Basic Hypothesis: Tyrosine phosphorylation of PCNA is a cancer-specific regulator of DNA repair. This project will test the role of receptor tyrosine kinases in PCNA phosphorylation and assess the pharmacologic targeting of nuclear tyrosine kinases.

Progress on Original Statement of Work: The original start of the project on all aims was delayed 6 months due to change of personnel and recruitment of new associates to fill out a full team. The overall progress during the specific reporting period now represents the proposed total effort. Major objectives of the proposed research plan have been achieved through further refinement and strategic definition of approaches to meet the technical challenges while contributing to the emerging knowledge of the roles of PCNA in breast cancers.

Aim 1a. To evaluate candidate tyrosine kinases potentially represented in the nucleus of tumor cells for their capacity to selectively target a unique sequence in PCNA including Y211.

Task 1. Recombinant expression and purification of different tyrosine kinases.

See Appendix 1: Task completed. This task had to take on many technical challenges and caused some delays before being fully optimized. The protocol for recombinant human PCNA was fully standardized as documented in the Appendix 1. Further efforts to pursue specific recombinant tyrosine kinases were channeled to other aspects of the project and instead commercial sources were used.

Task 2. Synthesis of the unique peptide sequence modeled after PCNA (containing Y211)

See Appendix 3: Task completed. A minimal set of peptides based upon the Y211 phosphorylation site in PCNA have been prepared for study. However, during the course of this project period there was publication of work which indicates that these particular studies would be redundant. Therefore the biochemical studies were de-prioritized and focused more on Aim1b.

Task 3. Development of an endpoint assay to measure pY211/Y211 levels using capillary electrophoresis

Task 4. Determine basic turnover kinetics using capillary electrophoresis

These two tasks 3 and 4 are tightly related and preliminary efforts have established feasibility of the capillary electrophoresis methodology. As indicated above, the overall approach has been de-prioritized and will be reserved for specific kinase and inhibitor studies based upon the results of Aim 1b and 2.

Aim 1b. To evaluate the nuclear kinase activities responsible for phosphorylation of PCNA at Y211 in tumor cell models.

Task 1. Growth and maintenance of breast cancer cell lines with and without inhibitor added

See Appendix 5: Task completed. The overall collection of tumor cell lines represents suitable diversity in breast disease models. However, the differences in growth rates and overall characteristics required careful implementation to be able to screen compounds across the panel and compare results. As a result, the panel of cell lines to test was reduced to 7 from the originally proposed 9 to meet cost and practical requirements. The cell panel was deployed to screen the novel synthetic compounds enabled in Aim 2.

Task 2. Prepare nuclear extracts of breast cancer cell lines using sucrose gradient

See Appendix 2: Task completed. This effort has been accomplished and used in both Aims 1 and 2.

Task 3. Perform Western Blot analysis, investigating expression of select nuclear tyrosine kinases

See Appendix 2: This task is completed but not through direct Western blotting in the tumor cell lines. What emerged over the course of the investigation was new information that warranted a more direct survey of protein kinase inhibitors in the context of PCNA phosphorylation. An alternative approach was developed to assess the impact of a panel of kinase inhibitors on Y211-phospho-PCNA in the context of cell cycle and in response to DNA damage.

Task 4. Determine the ability of the unique peptide sequence to be phosphorylated in nuclear extracts of breast cancer cells with and without inhibitors

This task was abandoned in lieu of evidence regarding the parameters dictating substrate specificity in the context of chromatin-bound PCNA.

Summary of Aim 1: The objectives for the overall aim were initially explored and adjusted as new information became available in the field regarding the particular subject of PCNA Y211 phosphorylation. The optimized purification of a stable trimeric PCNA preparation enabled initial pursuit of preliminary phosphorylation studies. These biochemical studies were originally designed to assess the correlation with reported cellular studies using antibody based affinity pull-down and Western blot analyses. The first survey studies with traditional ATP consumption assays using epidermal growth factor receptor, the putative kinase that targets the

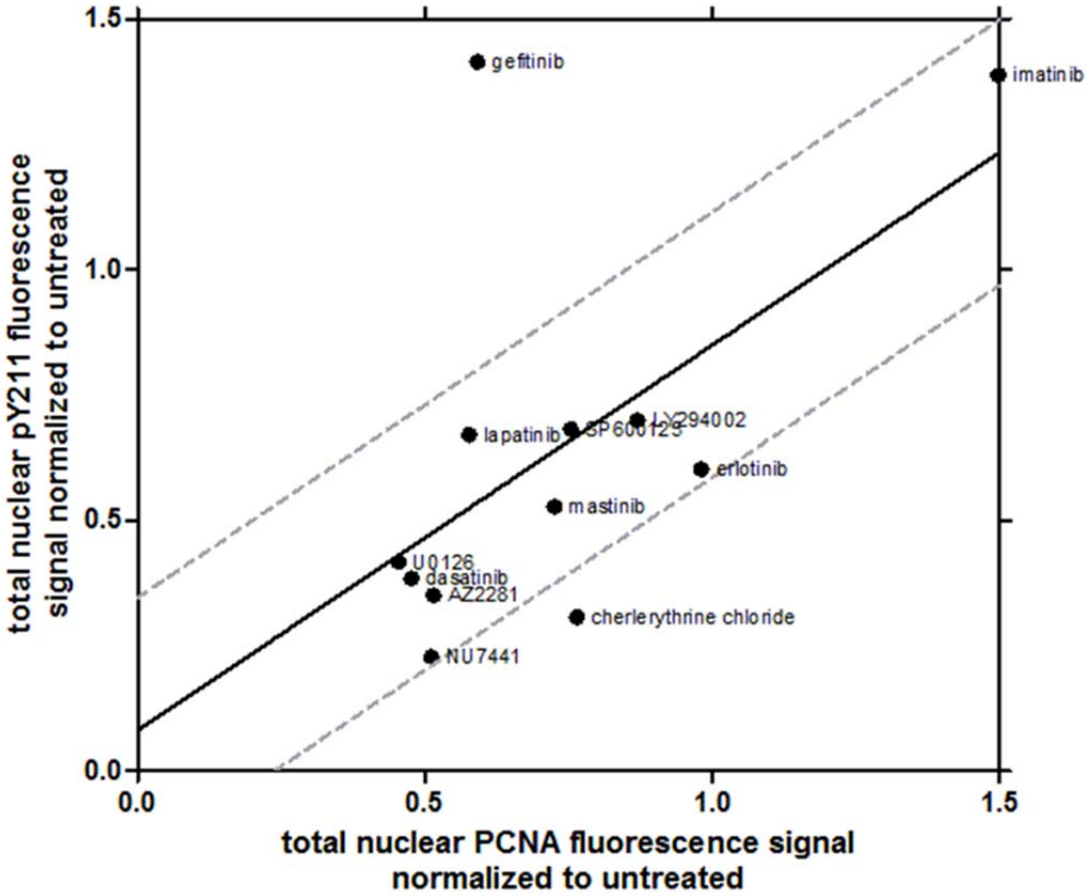

Figure 1. **The relative impact of protein kinase inhibitors on synchronized breast tumor cells MDA-MB-468**. Linear Regression: y=0.7679x+0.08144, R^2 = 0.3382 (solid line); dashed lines represent the standard deviation of the linear regression (y-intercept value: 0.2647). It is clear that gefitinib, erlotinib, cherlerythrine chloride, and NU7441 should be retested to verify the profoundly distinct effects on Y211-PCNA content.

Y211[1]. A secondary report from the same laboratory implicated Abl kinase and this was also pursued using in vitro biochemical methods[2]. The results were not consistent with what was observed in vitro.

Given the overall challenges with peptide substrates for kinases not reflecting preferential selectivity, it became evident that a critical assessment for translational impact would be difficult. The implications from these efforts are that the observations regarding cellular kinases operational on PCNA could require specific context of a protein context bound to chromatin. As a result, the *in vitro* biochemical experiments in Aim 1a were de-emphasized and the efforts were shifted to Aim 1b and Aim 2.

The tasks associated with this Aim 1b were modified to further address the insights gained from the *in vitro* studies. These modified objectives take into account he emerging literature regarding post-translational modifications of PCNA. A redesign of the primary experiment expanded the scope of the question to be addressed in Aim 1. The relevant issues for translation are: a) what pathways are leading to PCNA-Y211 phosphorylation, and b) can deployment of existing kinase inhibitors modulate the functional status of PCNA. A related but critical point is whether Y211-phosphorylation is sufficient or necessary for a full DNA damage response.

For both questions, the appropriate analytical methods to detect the changes in the Y211-PCNA nuclear compartment are required. The progress to date on this Aim is focused on methods development and implementation along with promising results (Figures 1 and 2). The details for these experiments are included in Appendix 2. Methods for subcellular fractionation are included as part of Aim 2 of tumor cells are implemented and validated in Appendix 6.

Assay Design 1: The kinase(s) responsible for PCNA phosphorylation remain weakly established and the current pathway associations are called into question. There are likely associations between upstream cell signaling pathways and different roles of PCNA in cell cycle. A series of protein kinase inhibitors each with different pathway preferences were used to assess the relative contributions to Y211 phosphorylation. Using serum starved cultures of triple-negative breast tumor cells, the relative impact of kinase inhibitors on the PCNA content and Y211-PCNA contents were investigated. After 24 h treatment, cells were harvested, lysed, and protein extracts were analyzed by Western blotting using antibodies for total PCNA, and Y211-PCNA. The results are presented in Figure 1 as a ratiometric analysis of change in total PCNA vs Y211-PCNA content.

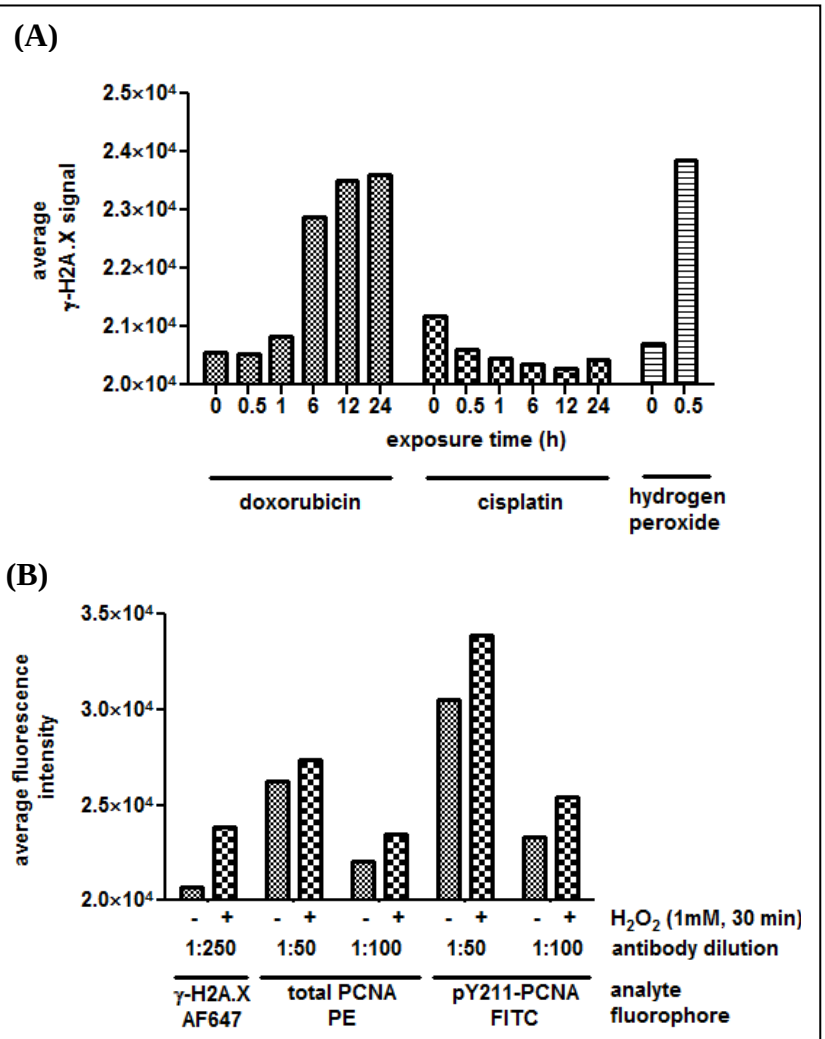

Figure 2; DNA Damage Responses of MDA-MB-231 Adherent Cell Lines. (A) Doxorubicin (1μM) and cisplatin (300μM) were incubated with 50,000 MDA-MB-231 cells for varying lengths of time before being fixed, permeabilized, and stained for pSer139-γH2A.X (Alexa647 conjugated antibody). **(B)** Three different markers (analytes) were analyzed in MDA-MB-231 cells that were treated for 30 minutes with 1 mM hydrogen peroxide before being fixed, permeabilized, and stained for pSer139-γH2A.X, pY211-PCNA, and total PCNA.

The data obtained from these studies are a rich information set that shed new perspective upon the subject of PCNA phosphorylation based upon what is in the current literature reports. A result with the EGFR tyrosine kinase inhibitor erlotinib indicates that some suppression of the Y211-PCNA can be effected without impact on total PCNA. Based upon the original observation[1], the result is largely consistent with what is expected. In contrast, the related inhibitor gefitinib exhibited an opposite result. While this inhibitor does target EGFR, there are distinctly different secondary kinase targets known to be effected by gefitinib. The increased levels of Y211-PCNA implicate a drug-induced response network that activates PCNA pools. Given that these data are comparing chromatin-free vs bound PCNA, it is consistent with the Y211-PCNA pools all being localized on chromatin. Overall, the most striking result is the relative small changes in the PCNA content and Y211-PCNA that occur in response to the kinase inhibitors after release from cell cycle block. This is not completely unexpected given the relative

Assay Design 2: The second experimental approach focused on the role of Y211-PCNA in the DNA damage response networks. Three different mechanistic DNA damaging agents were used to assess their effects on the formation of nuclear foci and Y211-PCNA. The breast tumor derived cell line MDA-MB-231 is a human

triple-negative breast cancer cell line and is known to initiate a strong DNA damage response. Due to the nature of these cell line and the predominant signaling pathways and known chemoresistance, it is anticipated to model many the upstream signaling pathways that contribute to the overall change in PCNA phosphorylation at Tyr211.

Formation of nuclear foci was observed through expression of pS139-γH2A.X, a known marker for DNA damage and repair in response to doxorubicin, cisplatin, and hydrogen peroxide. Doxorubicin is known to cause single- and double-stranded breaks, cisplatin is known to initiate crosslinks between strands of DNA, and hydrogen peroxide causes alkylation of the nitrogenous bases on DNA. Based upon established literature, doxorubicin and cisplatin are known to take longer before a DDR is measured (6-24 hours) compared to hydrogen peroxide (10-30 minutes), and this could be directly contributed to the difficulty of a cell to efficiently repair the damage.

Implementation: A series of seven different molecular markers will be monitored and correlated with shifts in the expression levels of PCNA phosphorylation at Tyr211 using a high throughput flow cytometry-based assay. Mammalian cell cultures are dispensed into 96 well plates and treated with and without a kinase inhibitor for 24 hours prior to being exposed to a DNA damaging agent. The exposure time of the DNA damaging agent will be based on the time required to achieve maximal pSer139-γH2A.X signal. Cells treated without the damaging agent will be used as a positive control and the cells treated with the damaging agent alone will be used as a negative control. Cells will be fixed with 1.6% paraformaldehyde followed by permeabilization with iced cold absolute (100%) methanol, and triton extracted to reveal nuclear epitopes. Cells will be stained with fluorescently labeled primary antibodies for 16 hours at 4°C prior to being analyzed on the HyperCyt-CyAn automated flow cytometry platform. Average fluorescence intensity values of the first 1000 gated events were used for each marker under a specific condition and compared to changes in pY211-PCNA expression levels (after normalization to total PCNA). The normalization to total PCNA accounts for changes in the PCNA content due to DNA damage.

Using a 96-well plate for the assay, 90-100% cell detachment was observed compared to very low detachment success in 384 well plates. Cells were treated with TrylES Select (Gibco) buffer for 30 minutes at 37°C before being agitated. Cells were transferred to a conical bottom plate before being fixed, permeabilized, and stained. An optimized standard operating procedure was developed for the treatment, detachment, and staining processes.

Preliminary Results: The DDR response was stronger in MDA-MB-231 cells with the administration of doxorubicin for 6-24 hours (Figure 2a). There was no observable change in the pSer139-γH2A.X expression levels in cisplatin treated MDA-MB-231 cells. The results suggests that the concentration or exposure time of cisplatin is not optimized. Cisplatin has previously shown to have a strong effect on the formation of nuclear foci and pSer139-γH2AX expression. Total PCNA and pTyr211-PCNA levels were also measured in MDA-MB-231 cells upon damage with hydrogen peroxide. An increase in the expression of all three markers was observed as anticipated (Figure 2b).

Given that hydrogen peroxide treated and untreated cells represent the assays positive and negative controls, respectively, a Z' factor was calculated to be 0.428, indicating the possibility of obtaining quantitative results from the screen platform executed in 96-well plates. For the first time to our knowledge, adherent cell cultures can be screened in a multiplex assay for nuclear phospho-protein markers. This opens a significant avenue for replacing the Western blot approach (as show above) with higher content and higher throughput screens to assess the relative effects of kinase inhibitors.

What is evident is that the molecular networks controlling PCNA phosphorylation and the functional consequences deserve continued investigation. There is complexity to this system which is tightly regulated meaning that the changes in overall content of phosphorylated PCNA in breast tumor cells exist within a narrow range. Traditional antibody based methodologies are marginal at best for addressing this problem motivating alternative kinase inhibitors that show changes in a specific marker or set of markers can now be classified and further characterized by dose-response curves and assessing the relevant pharmacodynamic markers.

Aim 2a. Using a structure-based approach, known experimental therapeutics will be targeted to the nucleus in breast cancer tumor cell models by synthetic incorporation of nuclear-delivery features.

Task 1. Acquire necessary tyrosine kinase inhibitors
See Appendices 1 and 4: Task completed. This task was accomplished as part of Aim 1 and used further in the phenotypic growth assays as part of Aim 2. In addition, three novel analogs of the tyrosine kinase inhibitor gefitinib were synthesized and tested (Appendix 4). This compound serves as the precursor for convergence with the peptide and peptoid nuclear localization targeting sequences.

Task 2. Synthesize peptoid nuclear localization sequence
See Appendix 3: Task completed. The molecules have been successfully prepared and have been used for cell based uptake and phenotypic tumor cell growth assays. In addition, there have been a series of peptides synthesized based upon the PCNA sequence containing Y211 and tested in growth phenotypic assays.

Task 3. Validate the nuclear localization sequence does target the nucleus of the breast cancer cells
See Appendix 5: Task completed with additional follow up studies in process. The varied length series of polycationic peptoids and peptoid-peptide hybrids have been tested in uptake studies using fluorescence microscopy in live cell assay as well as for phenotypic growth effects on two breast tumor cell lines.

Task 4. Couple peptoid nuclear localization sequence to the tyrosine kinase inhibitor:
See Appendix 3: Task completed. Novel conjugates of the tyrosine kinase inhibitor gefitinib have been synthesized. Structural variants of the gefitinib tyrosine kinase inhibitor have been coupled to nuclear targeting peptides, cell penetrating peptoids, and hybrid peptoid-peptides.

Task 5. Perform colocalization studies using fluroescence microscopy to validate localization of inhibitor to the nucleus
See Appendix 5: Task completed but additional studies are warranted based upon the results and the ambiguity in the reported literature.

Task 6. Perform cell growth inhibition assays using breast cancer cell lines and the nuclear-localized tyrosine kinase inhibitors.
See Appendix 5. Task completed and data are reported showing that the gefitinib-peptoid conjugates retain significant growth inhibitory activities. These data warrant continued investigations into the kinase profiles being impacted by the inhibitor.

Aim 2b. Using novel, ultra-sensitive, quantitative Raman-based detection tools, the capacity of nuclear-targeted tyrosine kinase inhibitors to alter the PCNA pY211/Y211 content in breast tumor cell models will be pursued.

Task 1. Further develop FFE isolation and SERRS detection platforms for quantitative assessment of pY211/Y211 levels of PCNA
See Appendix 6. These efforts have continued through comparison of fluorescence and Raman based detection for ratiometric analysis.

Task 2. Prepare nuclear extracts of breast cancer cell lines using sucrose gradient
See Appendix 6. Task completed and also utilized in Aim 1.

Task 3. Separate nucelar protein extracts using FFE
See Appendix 6: Task completed and the feasibility of PCNA isoform separations has been documented.

Task 4. Perform dot blot analysis of the nuclear protein FFE fractions
See Appendix 6: This assay has been reduced to practice and is now modeled after a reversed-phase immunological assay using a high capacity PVDF membrane. This basic methodology of printing FFE fractions onto PVDF and use of specific antibodies to stain the membrane has been tested for use with both fluorescence and Raman based detection.

Task 5. Analyze pY211/Y211 levels of PCNA using SERRS detection
This task has not fully accomplished using SERRS but was evaluated using Western blots; additional studies and development of the platform are warranted.

Summary Aim 2: The primary progress on this Aim has been focused on sourcing of novel chemical agents that address the specific molecular design questions of nuclear targeting. The problem to be addressed was articulated in the original proposal and has largely remained the same. What has emerged since that time is an ever increasing level of significance to understanding and translating the role of nuclear kinases to control DNA damage repair pathways. When the project started, there was a great deal of skepticism about the concept that cytosolic kinases translocate to the nucleus. In addition, the broader substrate selectivity (and hence role) of nuclear kinases such as DNA-PK was only poorly defined. Given the efforts in Aim 1 regarding the use of kinase inhibitors to modulate phospho-PCNA, testing the approach of nuclear targeting of a kinase inhibitor through conjugation was pursued. Also, a report of a peptide derived from PCNA-Y211 having an impact on prostate cancer cell growth appeared. This observation warranted testing in the context of the triple negative breast tumor cell models.

In Appendix 5 is summarized the specific experimental aspects for synthesis of peptides and peptoids. These materials have been confirmed for mass content after purification by HPLC. There were many technical hurdles and some remain for the scalability of the synthetic preparations using solid phase. A great deal of effort continues to be put forth in improving the process and yield of the peptoid and peptoid-peptide hybrid. While these compounds have been tested for phenotypic growth inhibition, their utility is largely devoted to the preparation of conjugates with the kinase inhibitor.

These basic peptides and polycationic peptoids were labeled with fluorescein and used to assess the effect of structure on cellular uptake. There are examples of the data in Appendix 5. The leader sequences were selected after a careful review of the literature and consideration of ease of synthesis. For this reason, the two attributes desired of cellular uptake and nuclear delivery was kept separate in consideration. What was established is that the poly-7 and poly-9 lysine-peptoid showed distinctive improvements in uptake. At this time what is less clear and remains to be more carefully established is if conjugation of the TAT peptide with the peptoid promoted nuclear localization and the persistence in the nuclear compartment.

In addition to testing for cell uptake and potential localization, the peptide and peptoid constructs have been tested in a tumor cell phenotype assay (Appendix 5). A surprising result was published during the early stages of the research period[4] that claimed growth inhibitory activity for simple nuclear-targeted peptides based upon the Y211-PCNA peptide. This claim was difficult to believe given the short life time of peptides in cells but nonetheless we agreed was very important to validate. We prepared the peptides as well and fluorescently-labeled versions of

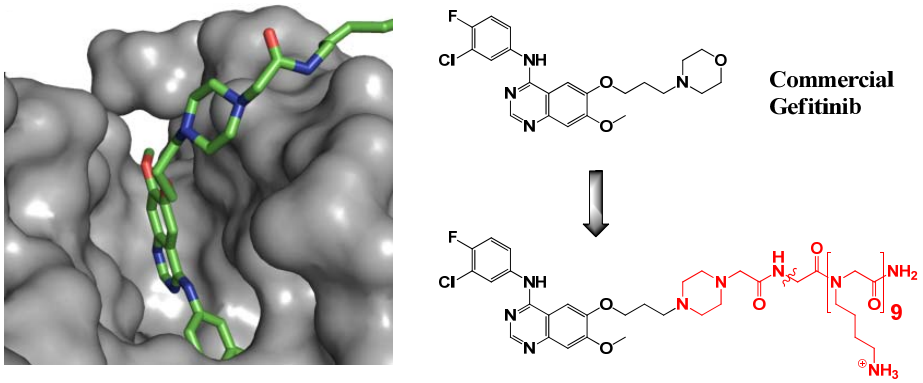

Figure 3. A docking model for the drug gefitinib in the EGFR kinase site. On the right side is the structural substitution of a peptoid conjugate that was synthesized during the project period. Additional types of analogs were prepared as well each providing sub-optimal performance for the chemical conjugation reactions or poor overall solubility of the product.

these molecules. Unfortunately, we were not successful in demonstrating significant nuclear delivery nor did we observe effects on the growth phenotypes of breast tumor cells. As a control, we elected to use the same cell types reported in the paper (prostate cell lines) and again were not able to detect a significant effect.

The original approach was based upon the use of the related inhibitor erlotinib. Based upon the chemical synthesis and respective biological profiles toward kinases, the approach was altered by selecting gefitinib as the core inhibitor. The docking model shown n Figure 3 along with the chemical drawings highlights the feasibility of a peptoid conjugate being able to bind in the EGFR active site.

A key kinase inhibitor analog has been made that is suitable for subsequent chemical modifications and inclusion of a nuclear localization sequence. This compound bears a close association with the commercial gefitinib but was modified to allow for inclusion of a spacer linker region that facilitated the overall conjugation (example in red Figure 3). While other alternative linkers and reactive groups were explored with gefitinib (see Appendices 3 and 4), there were problems with the solubility or reactivity for the conjugation reaction.

These gefitinib analogs (before conjugation) showed promising activity in the breast tumor cell growth phenotype assay. In fact, there was clear evidence that these molecules could be detected as cytotoxic (Figure 4 and Appendix 5). More importantly, after conjugation with a peptoid poly-lysine sequence (Figure 3), a significant level of activity in this assay was retained. Supporting this observation is the fact that a second hybrid conjugate with a nuclear-targeting (SV40) sequence had equivalent and significant growth inhibitory in chemoresistant, triple negative cell line MDA231, and cytotoxic activity in MDA468. Overall, the concept and use of these conjugate kinase inhibitors has been reduced to practice and offers potential to be further exploited in breast cancers. The motivation to move these forward warrants a scale up of the synthesis and further testing against additional breast tumor cell lines, and *in vivo* testing in a triple negative breast tumor xenograft model. All these objectives will be the subject of pursuit for future funded research studies.

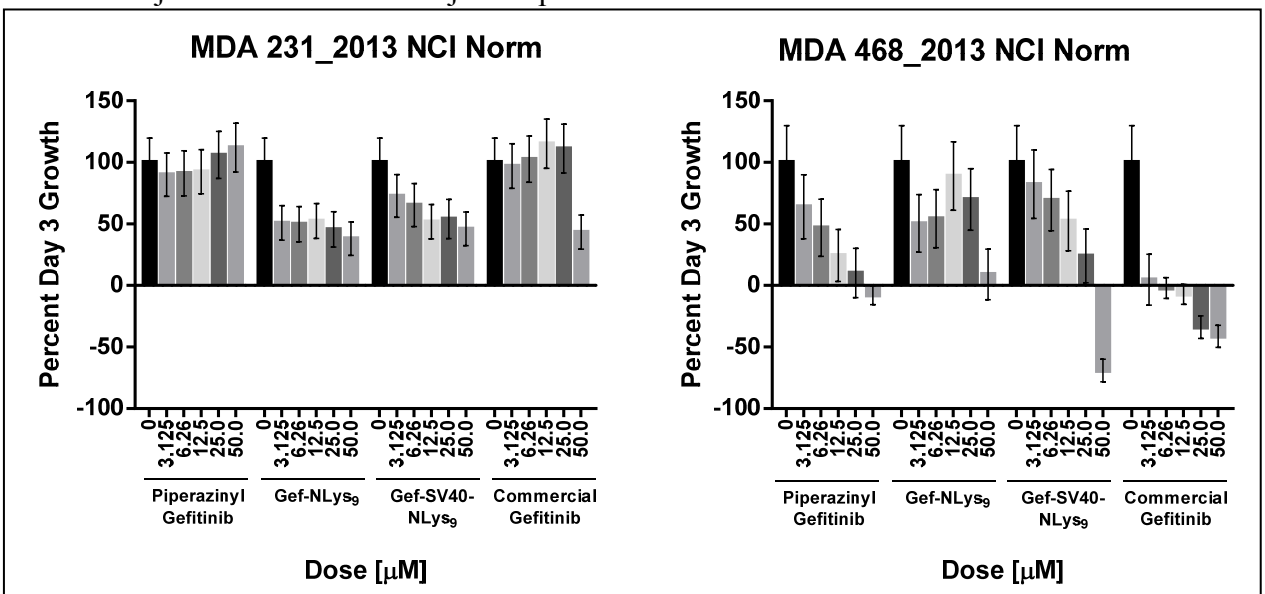

Figure 4. An example of the tumor cell growth inhibition and cytotoxicity induced by the gefitinib analogs and the peptoid conjugates (Appendix 3).

The second component of Aim 2 is focused on the technology development for improved sensitivity of protein isoforms of PCNA. The progress on this aim has been entirely focused on methods development and optimization for separation of PCNA protein isoforms, quantification using reverse immunological assays, and comparison with standard ELISA assays. As demonstrated in the Aim 1 studies in Appendix 2 Figure 2.7, PCNA fractions associated with chromatin have distinct differences in migration in SDS-PAGE. There is now a growing body of information about the roles of PCNA post-translational modifications especially in response to DNA damage[3]. However, accurate and multiplex methods for quantification of PCNA isoforms with the sensitivity needed for clinical samples have remained elusive.

A new labeling reagent process for production and scale up has been developed in-house that offers promise for efficient and ultrasensitive measurement of PCNA using Raman with surface enhancement

(Appendix 6). A high resolution pre-fractionation and separation method based free-flow electrophoresis has been implemented to assess the relative abundance of different PCNA isoforms in the nuclear compartment of cells treated with DNA damaging agents. Chromatin bound fractions are highly enriched with PCNA in cells after DNA damage response is elicited. A key question remains which forms of PCNA are the most relevant disease markers for the damage pathways in different breast tumors. This combination of a high throughput separation method followed by blotting on PVDF and immune-detection with Raman active dye-labeled antibodies offers a competitive and potentially superior detection technology to modern fluorescence based measurements.

KEY RESEARCH ACCOMPLISHMENTS:

-Synthesis and testing of a novel protein tyrosine kinase inhibitor-peptoid conjugates with inhibitory activity against triple negative human breast tumor cells.

- Biologically active receptor tyrosine kinase inhibitors contain suitable functionality for use in reaction to conjugate nuclear targeting sequences. The combination of a nuclear targeting peptide-peptoid hybrid with the receptor tyrosine kinase inhibitor also produced a novel entity with inhibitory activity toward the breast tumor cell lines.

-A panel of protein kinase inhibitor treatments of triple negative breast tumor cells has been shown to elicit differential impacts on total PCNA content and the ratio of Y211 phospho-PCNA in nuclear compartments.

-Quantitative data that demonstrates PCNA almost exclusive localization on chromatin in breast tumor cells after addition of protein kinase inhibitors or DNA damaging agents.

-DNA damage response markers correlate with the changes in PCNA and pY211-PCNA in a triple negative breast tumor model showing for the first time a connection in the response pathway.

-Feasibility of antibody labeling containing equal levels of isotopic variants of a Raman-active dye has been established.

-Proof of concept application of Raman-based detection combined with reverse immunological assays for quantification of cancer specific PCNA-isoforms has been accomplished.

-Using breast tumor cell nuclear proteome extracts, free-flow fractionation, and reverse-phase immunological assays, a diversity of PCNA isoforms have been detected with sensitivities exceeding those available with standard fluorescence.

REPORTABLE OUTCOMES:

Era of Hope 2011, August 2-5, 2011 poster entitled: “Targeting PCNA Phosphorylation in Breast Cancer” V. Jo Davisson, Anthony Pedley, Qingshou Chen, Matt Bartolowits, Kyle Harvey, Raymond Fatig.

A manuscript in preparation “Signaling to the Nucleus Involves Dynamic Changes in PCNA Isoform Content” outlines the use of quantitative ratiometric analysis of pY211-PCNA to PCNA in response to protein kinase inhibitors and DNA damaging agents. The experimental work entails results that link distinct cell signaling pathway inhibitors to the nuclear changes in pY211-PCNA content.

A manuscript in preparation: “The Design, Synthesis, and Biological Activities of Gefitinib-peptoid Conjugates”; additional experimental effort will be needed to define the robustness of the methods and the alteration in kinase inhibition profiles.

A manuscript in preparation on methodology for the use of reverse phase immunological assays for chromatin associated PCNA isoforms based upon novel surface-enhanced Raman detection technologies. “PCNA Isoform Quantification using Surface Enhanced Raman Methods”

CONCLUSION

A new perspective on the role of PCNA phosphorylation as an indicator of nuclear events in response to kinase signaling pathway inhibition has emerged. While expected to respond to DNA damage, the connection between PCNA pY211 and DNA damage response are also implicated. The potential for altering the kinase inhibitory pathway profile for gefitinib (Iressa) through conjugation with cell penetrating and nuclear targeting peptoids

has been established. Further investigation of the peptoid-peptide hybrid conjugates is warranted based upon the current results to assess the potential for translation in breast cancers. A new assay and detection technology coupled with proteome separation indicates a broader diversity of PCNA isoforms than expected and offers a new avenue to assess the translational significance.

REFERENCES:

1. Wang, S.-C. *et al.* Tyrosine phosphorylation controls PCNA function through protein stability. *Nat. Cell Biol.* **8,** 1359–1368 (2006).
2. He, X. *et al.* Proliferating cell nuclear antigen destabilizes c-Abl tyrosine kinase and regulates cell apoptosis in response to DNA damage. *Apoptosis Int. J. Program. Cell Death* **14,** 268–275 (2009).
3. Mailand, N., Gibbs-Seymour, I. & Bekker-Jensen, S. Regulation of PCNA–protein interactions for genome stability. *Nat. Rev. Mol. Cell Biol.* **14,** 269–282 (2013).
4. Punchihewa, C. *et al.* Identification of Small Molecule Proliferating Cell Nuclear Antigen (PCNA) Inhibitor That Disrupts Interactions with PIP-box Proteins and Inhibits DNA Replication. *J. Biol. Chem.* **287,** 14289–14300 (2012).
5. Zhao, H. *et al.* Targeting Tyrosine Phosphorylation of PCNA Inhibits Prostate Cancer Growth. *Mol. Cancer Ther.* **10,** 29–36 (2011).
6. Kalderon, D., Roberts, B. L., Richardson, W. D. & Smith, A. E. A short amino acid sequence able to specify nuclear location. *Cell* **39,** 499–509 (1984).
7. Frankel, A. D. & Pabo, C. O. Cellular uptake of the tat protein from human immunodeficiency virus. *Cell* **55,** 1189–1193 (1988).
8. Yoneda, Y. *et al.* Synthetic peptides containing a region of SV40 large T-antigen involved in nuclear localization direct the transport of proteins into the nucleus. *Exp. Cell Res.* **170,** 439–452 (1987).
9. Wychowski, C., Benichou, D. & Girard, M. A domain of SV40 capsid polypeptide VP1 that specifies migration into the cell nucleus. *Embo J.* **5,** 2569–2576 (1986).
10. Potocky, T. B., Menon, A. K. & Gellman, S. H. Cytoplasmic and nuclear delivery of a TAT-derived peptide and a beta-peptide after endocytic uptake into HeLa cells. *J. Biol. Chem.* **278,** 50188–50194 (2003).
11. Hodoniczky, J., Sims, C. G., Best, W. M., Bentel, J. M. & Wilce, J. A. The intracellular and nuclear-targeted delivery of an antiandrogen drug by carrier peptides. *Pept. Sci.* **90,** 595–603 (2008).
12. Rajendran, L., Knolker, H.-J. & Simons, K. Subcellular targeting strategies for drug design and delivery. *Nat. Rev. Drug Discov.* **9,** 29–42 (2010).
13. Pan, L. *et al.* Nuclear-Targeted Drug Delivery of TAT Peptide-Conjugated Monodisperse Mesoporous Silica Nanoparticles. *J Am Chem Soc* **134,** 5722–5725 (2012).
14. Wender, P. A. *et al.* The Design, Synthesis, and Evaluation of Molecules That Enable or Enhance Cellular Uptake: Peptoid Molecular Transporters. *Proc. Natl. Acad. Sci.* **97,** 13003–13008 (2000).
15. Umezawa, N., Gelman, M. A., Haigis, M. C., Raines, R. T. & Gellman, S. H. Translocation of a β-Peptide Across Cell Membranes. *J Am Chem Soc* **124,** 368–369 (2001).
16. Peretto, I. *et al.* Cell penetrable peptoid carrier vehicles: synthesis and evaluationElectronic supplementary information (ESI) available: experimental details. See http://www.rsc.org/suppdata/cc/b3/b306438g/. *Chem. Commun.* 2312 (2003). doi:10.1039/b306438g
17. Schröder, T. *et al.* Peptoidic Amino- and Guanidinium-Carrier Systems: Targeted Drug Delivery into the Cell Cytosol or the Nucleus. *J Med Chem* **51,** 376–379 (2008).
18. Unciti-Broceta, A., Diezmann, F., Ou-Yang, C. Y., Fara, M. A. & Bradley, M. Synthesis, penetrability and intracellular targeting of fluorescein-tagged peptoids and peptide–peptoid hybrids. *Bioorg. Med. Chem.* **17,** 959–966 (2009).
19. Mandal, D., Nasrolahi Shirazi, A. & Parang, K. Cell-Penetrating Homochiral Cyclic Peptides as Nuclear-Targeting Molecular Transporters. *Angew. Chem. Int. Ed.* **50,** 9633–9637 (2011).
20. Zuckermann, R. N., Kerr, J. M., Kent, S. B. H. & Moos, W. H. Efficient method for the preparation of peptoids [oligo(N-substituted glycines)] by submonomer solid-phase synthesis. *J. Am. Chem. Soc.* **114,** 10646–10647 (1992).

21. Yu, Y.-L. *et al.* Targeting the EGFR/PCNA Signaling Suppresses Tumor Growth of Triple-Negative Breast Cancer Cells with Cell-Penetrating PCNA Peptides. *Plos One* **8,** e61362 (2013).
22. Angell, Y. M., García-Echeverría, C. & Rich, D. H. Comparative studies of the coupling of N-methylated, sterically hindered amino acids during solid-phase peptide synthesis. *Tetrahedron Lett.* **35,** 5981–5984 (1994).
23. Hood, C. A. *et al.* Fast conventional Fmoc solid-phase peptide synthesis with HCTU. *J. Pept. Sci. Off. Publ. Eur. Pept. Soc.* **14,** 97–101 (2008).

Appendix 1: Production and Purification of Recombinant N-terminal $(His)_6$-PCNA Protein Purification

Background: The following information outlines the production and purification of N-terminal $(His)_6$-PCNA protein from transformed BL21(DE3) cells. Optimizing and validating the recombinant PCNA protein purification to avoid aggregation was a major technical hurdle. The objective was defined as stabilization of the trimeric form of the protein in solution while preventing higher order non-specific aggregation. Ultimately, the project subaim was limited in part by the technical problems encountered in working with recombinant PCNA. None the less, a suitable preparation for binding studies was deployed while the biochemical modification studies proved problematic.

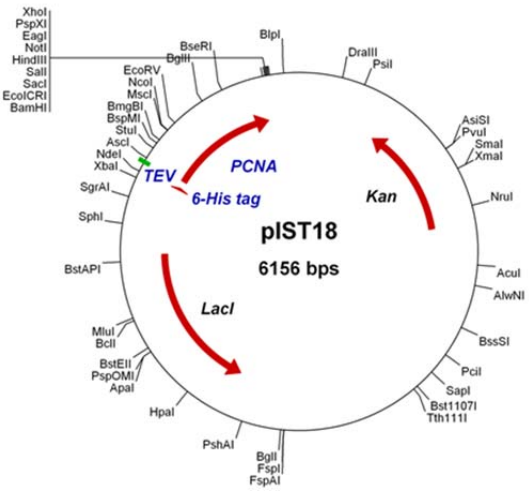

MHHHHHHSSGVDLGTENLYFQ|SNIGSGM…

Figure 1.1 The expression plasmid used to produce recombinant human PCNA in E. coli. The green coloration in the sequence is first codon of PCNA, the poly his-N-terminus is for affinity purification and the TEV cleavage site is marked by a vertical line.

One observation was that decreased trimer stability resulted in protein precipitation. Based on the possibility that the nickel-$(His)_6$ affinity tag interaction was the culprit, the $(His)_6$ affinity tag was removed by introducing the proteins to a unique TEV protease cleavage site (see plasmid Figure 1.1). The initial attempts at purifying recombinant PCNA yielded high recovery, but the protein readily aggregated in the absence of DTT and EDTA. Therefore, 1 mM DTT and 1 mM EDTA was introduced to the PCNA affinity purified fractions through dialysis for 6 hours. At that point, the protein started to visibly aggregate as determined by size exclusion chromatography, so addition of reducing agents and metal chelators temporarily decreased the protein aggregation (Figure 1.2). The results indicated that there was still a substantial amount of aggregated PCNA protein.

Another reduction agent, TCEP, was tried since it has a longer lifetime (24 hours versus 6 hours). Addition of 1 mM TCEP did not work as efficiently as DTT. It was hypothesized that the free nickel is bound to the affinity tag causing the protein precipitation. Metal-protein interactions have been known to initiate protein precipitation and the dissociation constant between immobilized nickel and histidine is approximately 1 uM. DTT is also known to reduce the chelating ability of nickel in solution whereas TCEP does not. Protein addition through Chelex resin also did not change the stability of PCNA in solution. Based on the possibility that the nickel-(His) affinity tag interaction was the culprit, the (His) affinity tag was removed by proteolysis. The results indicated that there was still a substantial amount of aggregated PCNA protein.

A recent publication outlining a new purification scheme for human PCNA was published during the course of the project[4]. This work published the first high throughput screen of chemical libraries for PCNA antagonists. The significant difference in the purification protocol was that after affinity chromatography, the protein was subjected to hydrophobic interaction chromatography using a phenyl sepharose column. Based on our results, the addition of sulfate into the protein system seemed to have a stabilizing effect on the PCNA trimer.

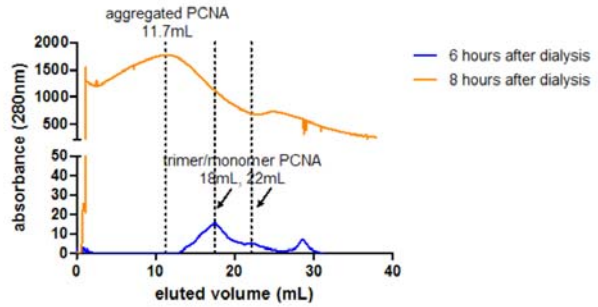

Figure 1.2 Aggregation of Recombinant PCNA Protein. Aggregation of recombinant PCNA protein was monitored by size exclusion chromatography on an automated AKTA FPLC system at 4 C. Trimer and monomer elution times were determined from a standard curve of protein standards.

An advantage of the new procedure is that the protein purification scheme can be scaled up with minimal sample handling. More importantly, the purification of PCNA can be performed in a day. However, thorough dialysis of the protein into HEPES buffer to remove all excess DTT, EDTA, and ammonium sulfate taking up to 48 hours is required. We made observation that prolonged exposure of the PCNA protein to ammonium sulfate will

cause PCNA to precipitate over the course of a week. Extensive dialysis is also needed to reduce interference in protein standardization methods (Bradford assay, UV-Vis spectroscopy) by DTT and ammonium sulfate. Using this improved, reproducible purification strategy, a yield of 5-7 mg/L culture was obtained (Figure 3.3). The extensive efforts to optimize production of functional PCNA are documented in a standard operational protocol as outlined below.

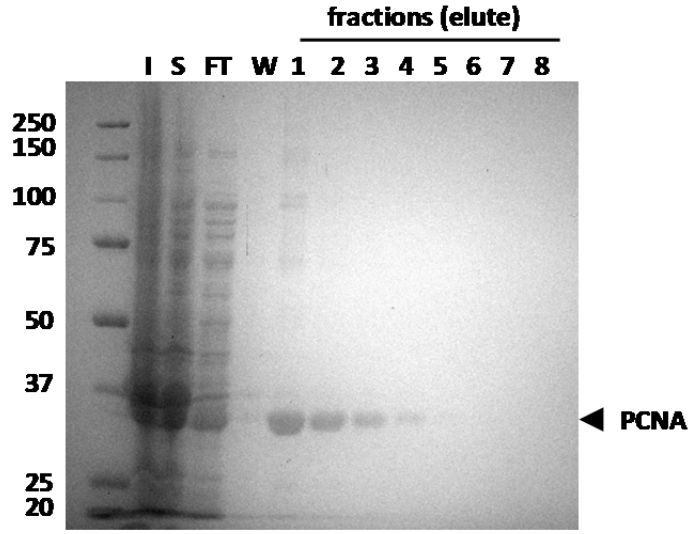

Figure 1. 3 Purification of N-terminal (His)-PCNA Protein by Affinity Chromatography. Analysis of the expression and affinity purification steps was analyzed by SDS-PAGE. SDS-PAGE imaged on a BioRad Gel Documentation platform after GelCode Blue staining. All protein standards are in terms of kDa. L=ladder (protein standards), I = insoluble fraction after lysing cells, S = soluble fraction after lysing cells, FT = flow through during purification process, W= wash during purification process.

Standard Protocol

A. *Long Term Reagent Storage of pellets*

Supplies and reagents are stored in different locations. Cell pellets of N-terminal $(His)_6$-PCNA transformed BL21(DE3) *E. coli* cells are located in the -80°C freezer. All buffers for the protein purification process are stored in the refrigerator. All columns should be stored in 20% ethanol and in the refrigerator or cold room (4°C).

B. *Reagent Recipes*

For the most part, these buffers can be kept in the refrigerator for a long period of time. Please note that Tris may start to precipitate out of solution. If at any point, the solution looks cloudy or a precipitate has formed, then discard the solution and make fresh. All imidazole elution solutions are only good for a short period of time. Do not use these solutions if they are older than a week.

E. coli Cell Pellet Lysis Buffer

25mM Tris buffer, pH 8.0

1mM 2-mercaptoethanol (add fresh, see note below)

To prepare a 1L solution of 25mM Tris buffer at pH 8.0, dissolve 3.03g into 900mL of deionized water. Adjust the pH by adding 1N NaOH drop-wise. Adjust volume to 1L with the addition of deionized water.

When it comes time to lyse the cell pellet, transfer 40mL of the 25mM Tris buffer at pH 8.0 to a cell pellet and add 3uL of 2-mercaptoethanol (β-mercaptoethanol or β-ME). Resuspend the pellet.

Affinity Chromatography Equilibrium Buffer

25mM Tris buffer, pH 8.0

20mM imidazole

To prepare a 50mL solution of 20mM imidazole in 25mM Tris buffer at pH 8.0, dissolve 68mg into 50mL of 25mM Tris buffer at pH 8.0. Mix until all the imidazole has dissolved.

Affinity Chromatography Elution Buffer

25mM Tris buffer, pH 8.0

1M imidazole

To prepare a 50mL solution of 1M imidazole in 25M Tris buffer at pH 8.0, dissolve 3.4g into 50mL of 25mM Tris buffer at pH 8.0. Mix until all imidazole has dissolved (may take a little time).

Ammonium Sulfate Stock Solution

25mM Tris buffer, pH 8.0

2M ammonium sulfate

To prepare a 50mL solution of 2M ammonium sulfate in 25mM Tris buffer at pH 8.0, dissolve 13.2g into 50mL of 25mM Tris buffer at pH 8.0. Mix well until all ammonium sulfate has dissolved (may take a little time).

Dialysis Buffer
25mM HEPES, pH 7.4
10% glycerol
0.01% Triton X-100
To prepare 2L of dialysis buffer, dissolve 11.9g of HEPES in 1L of water. Add in 200mL of glycerol and 200uL of Triton X-100. Stir until all has been incorporated. Add another 1L of water and adjust the pH to 7.4.

Column Regeneration Solutions
Solution 1: 1M NaOH. To prepare 50mL of a 1M NaOH solution, dissolve 20g of sodium hydroxide pellets in 500mL of water. Stir vigorously with a cap on to prevent splashing. Note: this solution may get warm.
Solution 2: 50mM EDTA. To prepare 50mL of a 50mM EDTA solution, dissolve 730mg of EDTA into 50mL of water. Mix well.
Solution 3: 100mM nickel sulfate. To prepare 50mL of a 100mM nickel sulfate solution, dissolve 1.31g of nickel (II) sulfate hexahydrate into 50mL of water. Mix well.

C. Procedures

In the following section, two different procedures are outlined. The first procedure is for the batch affinity purification of N-terminal $(His)_6$-PCNA using Ni-NTA resin. The second procedure is for the column-based affinity purification of N-terminal $(His)_6$-PCNA using a preassembled 3 mL column. The column was assembled using Ni-NTA chelating resin purchased through ThermoScientific. The column volume is 3 mL. Take note to the bold headings to indicate what method the procedure is being used.

For both procedures (batch and column)
Lysis Protocol for Generation of Soluble, Clarified Protein Lysate
1. Remove a 1L *E.coli* pellet from the -80°C freezer. Allow to thaw on ice. This process may take up to 2 h.
2. Add 20mL of lysis buffer to the pellet and mix to resuspend the pellet. Place pellet back on ice.
3. Turn on the sonicator by flipping the switch on the back of the instrument and place the probe into the resuspended pellet. Keep the resuspended pellet on ice.
4. Program the method on the sonicator so that there is a 3 minute processing time with 20 seconds on and 20 seconds off time. Also set the amplitude at 3 (30%). Do not set above 4 (or 40% without notifying everyone in the lab and proper ear protection).
5. Start the method by pushing the Start button.
6. After completion of the method, turn off the sonicator by flipping the power switch at the back of the instrument.
7. Remove the probe sonicator from the lysate and wipe down with 80% ethanol.
8. Transfer the lysate between 2 Oakridge tubes.
9. Centrifuge the lysate at 4,000×*g* for 20 minutes at 4°C.
10. Transfer the supernatant to a fresh 50mL Falcon tube and place on ice. This is the clarified protein lysate to use in the next steps.

Batch-based Affinity Chromatography Procedures
Loose Ni-NTA resin is not stored. This was used a few times for ease of scalability, but since then a column has been the preferred method for purifying.

Regeneration of Ni-NTA Affinity Resin
1. Transfer the used Ni-NTA resin into a 1.5mL Eppendorf tube. Centrifuge if necessary to pellet the resin if the volume of the slurry is larger than 1mL.
2. Centrifuge the Ni-NTA resin for 1 minute at 4000×*g* using a benchtop ultracentrifuge.
3. Decant off the supernatant and add 1mL of 1M NaOH. Mix well and incubate for 2 minutes at room temperature.

4. Centrifuge the Ni-NTA resin for 1 minute at 4000×*g* using a benchtop ultracentrifuge.
5. Wash the resin twice with deionized water, making sure to resuspend the resin.
6. Decant off the supernatant and add 1mL of 50mM EDTA. Mix well and incubate for 2 mintues at room temperature.
7. Centrifuge the Ni-NTA resin for 1 minute at 4000×*g* using a benchtop ultracentrifuge.
8. Decant off the supernatant and wash the resin twice with deionized water making sure to resuspend the resin.
9. Add 1mL of 100mM nickel sulfate to each Eppendorf tube with pelleted resin. Mix well and incubate for 2 minutes at room temperature.
10. Centrifuge the Ni-NTA resin for 1 minute at 4000×*g* using a benchtop ultracentrifuge.
11. Wash the resin twice using deionized water, making sure to resuspend the resin.
12. Wash the resin twice with 20% ethanol (for storage) or equilibration buffer for immediate purification.

Batch Purification by Affinity Chromatography

1. Regenerate the Ni-NTA loose resin, if not previously done. See above for procedure.
2. Add the soluble, clarified protein lysate to a 50mL Falcon tube containing 1mL Ni-NTA loose resin.
3. Attach the 50mL Falcon tube on a nutating mixer for 2 hours at a speed of 20rpm.
4. After 2 hour incubation, remove the Falcon tube and centrifuge at 400×*g* for 8 minutes at 4°C.
5. Remove the supernatant and put into a 50mL Falcon tube. Label the tube as flow through.
6. Add 5mL of equilibration/wash buffer to the resin and resuspend. Centrifuge the tube at 400×*g* for 8 minutes at 4°C.
7. Remove the supernatant and repeat step 6 two more times or until a negative Bradford test is observed. See below for procedure for Bradford test.
8. Add 2mL of elution buffer to the resin and mix briefly on a vortex mixer. Leave on ice for 2-3 minutes.
9. Centrifuge the tube at 400×*g* for 8 minutes at 4°C.
10. Remove the supernatant and repeat steps 8 and 9 until a negative Bradford test is observed.

Bradford Test to Observe Protein Elution

1. Prepare 10mL of a 1X Bradford dye. Pipet 1.6mL of 5X Bradford dye into 8.4mL of water. Mix well.
2. To 200µL of 1X Bradford dye, add 10µL of the eluted protein sample.
3. Mix well and observe color change. If the solution turns blue, continue with elution (or washes) until a negative results is observed.

Column-based Affinity Chromatography Procedures

It is very important that when using the column, do not let the column go dry and always clean the resin after usage. Do not store it in water or any buffer. There is a big probability that bacterial contamination may occur, and this would eliminate any growth if performed properly.

Regeneration of Ni-NTA Affinity Resin

1. Add 5 column volumes of water to the stored resin solution (20% ethanol).
2. Add 2 column volumes of 1M NaOH. Allow the solution to go through the column.
3. Rinse the resin with 5 column volumes of deionized water and allow the water to go through the column.
4. Add 2 column volumes of 50mM EDTA. Allow the solution to go through the column.
5. Rinse the resin with 5 column volumes of deionized water and allow the water to go through the column.
6. Add 2 column volumes of 100mM nickel sulfate and allow the solution to go through the column. At this point, the resin should turn a teal/blue color and the flow through solution will turn blue.
7. Rinse the resin with 2 column volumes of deionized water and allow the water to go through the column.
8. Rinse the resin with 2 column volumes of 25mM Tris buffer at pH 8.0 unless the column is ready to be stored. If it is ready to be stored, add in 4-5 column volumes of 20% ethanol in deionized water.

Column Purification by Affinity Chromatography

1. Regenerate the Ni-NTA resin, if not previously done.
2. Add the soluble, clarified protein lysate to the affinity column and allow the protein to go through the column. Make sure to collect the protein in a 50mL conical tube. Label this tube as flow through.
3. Wash the resin with 5 column volumes of water.
4. Wash the resin with 5 column volumes of 20mM imidazole in 25mM Tris buffer at pH 8.0. Collect the flow through in a 50mL conical tube and label as wash. After 5 column volumes, perform a quick Bradford test to see if protein is still eluting off of the column. If not, then continue on. If there is still protein eluting off of the resin, then add more equilibration buffer. Procedure for performing the Bradford assay can be found in the batch purification procedure section.
5. Elute off the protein starting with 2 column volumes of elution buffer. Collect all eluted protein in a 50mL conical tube labeled as eluted protein. After 2 column volumes, perform a quick Bradford test to see if protein is still eluting off of the column. If not, then continue on. If there is still protein eluting off of the resin, then add more equilibration buffer. Procedure for performing the Bradford assay can be found in the batch purification procedure section.
6. Once no more protein is being eluted off of the column, then regenerate the column and store properly.

For both procedures (batch and column)

Analysis of PCNA Purification and Dialysis

1. Remove 20µL of each fraction (eluted) and place into individually labeled Eppendorf tubes.
2. Combine all fractions that showed the presence of protein by Bradford test into a 50mL Falcon tube. Add in the necessary amount of DTT and EDTA to yield a final concentration of 1mM.
3. Adjust the combined protein fraction solution with the 2M ammonium sulfate stock solution.
4. Place the protein solution at 4°C on a nutating mixer for 1 hour at a speed of 20rpm.
5. After the 1 h incubation, transfer the contents to a prewet dialysis tube. If there are a lot of visible solids, the recovery is not going to be great. I would suggest that it is not really worth your time to continue. Just start over with a new pellet. At this point, PCNA is normally greater than 90% pure, so if there is visible precipitation, most of the protein is lost. One suggestion that has worked a little in the past is just to add even the precipitate to the dialysis tube. As the excess ammonium sulfate is removed, the protein may go back in solution and refold. However, this will require a lot of additional confirmation analyses and time.
6. Dialyze the contents for at least 2 days, making sure to exchange the buffer after 2 and 4 hours.
7. After dialysis, remove the contents of the dialysis tube and centrifuge at 2,000×*g* for 10 minutes at 4°C, and remove the supernatant.
8. Quantify protein by UV-Vis using an extinction coefficient of 14,800 $M^{-1}cm^{-1}$.
9. Concentrate the lysate using a prewet 10,000 MWCO spin filter, if needed.
10. Determine purity by SDS-PAGE. Make sure to include all sample aliquots in order to observe the efficiency of the purification.

Appendix 2. Breast Tumor Cell Line Panel and Kinase Inhibitor Screen

The following cell lines have been acquired, in cultivation, and are currently available for testing.

Table 2.1

cell line	HER2	ER	PR	p53	BRCA1
SKBR3	+	-	-	mutant	WT
MDA-MB-231	-	-	-	mutant	WT
MDA-MB-468	-	-	-	mutant	WT
MCF7	-	+	+	WT	WT
BT474	+	+	+	WT	WT
UACC812	+	+	-	WT	WT
ZR75B	-	+	-	WT	WT
HCC1569	+	-	-	WT	WT
HCC1937	-	-	-	WT	5382insC
T47D	-	+	+	mutant	WT

Tyrosine Kinase Inhibitors Acquired

The following table is a compilation of all the tyrosine kinase inhibitors were acquired (13 total). These compounds were formulated and used for the proposed cellular analyses (see table below). The molecular target listed may not be the only target for the kinase inhibitor. Most kinase inhibitors act almost like pan kinase inhibitors at high concentrations.

Table 2.2

flask	kinase inhibitor	kinase targeted	comments
1	untreated	--	
2	erlotinib	EGFR	noticed higher cell numbers
3	gefitinib	EGFR	noticed higher cell numbers
4	lapatinib	EGFR/ErbB2	noticed higher cell numbers
5	imatinib	c-Src	
6	dasatinib	c-Abl	
7	mastinib	c-Kit	
8	LY294002	PI3K	
9	U0126	MEK	
10	SP600125	JNK	
11	cherlerythrine chloride	PKC	cell death?
12	NU7441	DNA-PK	
13	AZD2281	PARP1	

Key: ER: estrogen receptor, PR: progesterone receptor, +: overexpressed, -: not overexpressed, WT: wild type

Detection of PCNA Phosphorylation upon Kinase Inhibitor Treatment in MDA-MB-468 Breast Cancer Cells

A panel of 12 different kinase inhibitors will be evaluated for their ability to alter the phosphorylation status of PCNA in MDA-MB-468 breast cancer cells. The objective is to identify those protein kinase-dependent pathways capable of modulating PCNA phosphorylation. The phosphorylation of PCNA was determined by an immunoprecipitation of PCNA after lysis of treated MDA-MB-468 breast cancer cells.

Cell Culture and Fractionation

All cell culture work was performed through the Purdue Center for Cancer Research Molecular Discovery and Evaluation Shared Resource Center (Ray Fatig). MDA-MB-468 breast cancer cells were grown to 60-70% confluence and split into individual T75 until 5.0×10^6 cells/flask. Cells were *serum starved* for 24 hours prior to drug treatment in the presence of FBS. All cells were treated for 24 hours at 10 μM drug.

Cell Harvest and Fractionation

Cells were harvested and lysed immediately to afford cytoplasm, chromatin unbound and bound nuclear fractions. Cell lysates were cleared through centrifugation ($2000\times g$) for 5 minutes at 4°C. Total protein concentration of each fraction was determined through a standard Bradford assay.

The following buffer recipe is a combination of recipes from *Short Protocols in Molecular Biology* and Wang, S-C.[1]. This recipe will produce three separate protein fractions: a cytosolic protein fraction, a chromatin-unbound (Triton-extractable) fraction, and chromatin-bound (Triton-resistant) fraction. The cytosolic and

chromatin-unbound nuclear fractions will be discarded for this analysis. Concentrating the protein will be performed prior to running on FFE to load as much protein as possible at a time.

Lysis Buffers to Prepare
Make sure to add the protease and phosphatase inhibitors at the last minute. Each buffer should remain ice cold during the process.

1. Initial Lysis Buffer: 20mM HEPES (pH 7.5); 0.25M sucrose, 3mM $MgCl_2$, 0.5% NP-40; 1mM DTT; 1X Halt protease inhibitor cocktail.
2. Nuclear Lysis Buffer (Triton): 10mM PIPES (pH 6.8), 100mM NaCl, 300mM sucrose, 3mM $MgCl_2$, 1mM EGTA, 0.2% Triton X-100, 25mM NaF, 2mM Na_3Vo_4, 5mM PMSF, 1X Halt protease inhibitor cocktail.
3. RIPA Lysis Buffer (SDS): 50mM Tris (pH 7.5), 150mM NaCl, 1% NP-40, 0.5% deoxycholate, 0.1% SDS, 25mM NaF, 2mM Na_3VO_4, 5mM PMSF, 1X Halt protease inhibitor cocktail.

Lysis Protocol to Isolate Chromatin-Bound Lysate

1. Resuspend 1.0×10^8 MCF7 breast cancer cell lines in 1mL of 1X PBS (pH 7.4). Transfer 500uL of resuspended cells to 2 separate Eppendorf tubes. Centrifuge the sample at 3000 rcf at 4°C for 5 minutes. Remove supernatant.
2. Resuspend the cells in 20X pellet volume of ice cold initial lysis buffer by gently pipetting up and down. Avoid doing this very fast as shearing of the cells may occur.
3. Use a 2.0mL Dounce homogenizer with pestle B to break the cells for 10 strokes, then transfer to a 1.5mL Eppendorf tube.
4. Centrifuge the sample at 3000 rcf at 4°C for 5 minutes. Remove supernatant (cytosolic fraction). Wash cell pellet three times with initial lysis buffer.
5. Resuspend the nuclear pellet in 2X pellet volume of nuclear lysis buffer by gently pipetting up and down. Centrifuge the sample at 3000 rcf at 4°C for 5 minutes. Discard the supernatant (chromatin-unbound fraction).
6. Resuspend the nuclear pellet in 2X pellet volume of RIPA lysis buffer and allow it to incubate for 5 minutes on ice.
7. Sonicate the sample using a probe sonicator every 10 seconds for 1 min on ice at an amplitude of 30.
8. Centrifuge the sample at 10,000 rcf for 10 minutes at 4°C. The supernatant will be the chromatin-bound protein fraction.
9. Perform a Bradford assay to determine protein concentration.

Bradford Assay and Total Protein Levels amongst Kinase Treatments The Bradford assay to determine total protein concentration amongst the various cellular fractions was performed. Briefly, 200 uL of 1X Bradford protein dye (BioRad) was added to each well, and 10uL of a 1:50 dilution of each sample was added to the corresponding well (n=3). In addition, a standard BSA curve was performed in order to correlate A_{595} values with protein concentration by means of a standard curve. Changes in A_{595} were determined by a simple plate read on a SpectraMax plate reader, and data analysis was performed in Microsoft Excel. Visualization of the standard BSA curve was performed in GraphPad Prism.

Table 2.3

Amount of Protein in Each Cellular Fraction

flask	kinase inhibitor	amount of protein (ug)		
		cyto.	chr. unbd.	chr. bd.
1	untreated	1374	836	598
2	erlotinib	1430	375	857
3	gefitinib	1489	863	619
4	lapatinib	1146	549	518
5	imatinib	1448	1359	889
6	dasatinib	1413	1285	651
7	mastinib	1306	1123	950
8	LY294002	1325	1511	665
9	U0126	1357	1300	1096
10	SP600125	1473	1278	952
11	cherlerythrine chloride	968	135	689
12	NU7441	1692	1385	768
13	AZD2281	1481	1239	1171

Preparation of Samples for SDS-PAGE
All samples were prepared at the same concentration in 1X SDS loading buffer. A total of 15uL of sample was added to each lane. This would represent a total of 10ug of protein per

lane (exception being the recombinant standard: 2ug loaded). Remanding sample was frozen at -80°C in case further analysis needs to be performed.

To accommodate all the samples, 2 precast Bis-Tris gels were used. Lane assignments are shown below.

	1	2	3	4	5	6	7	8	9	10	11	12	13	14	15	16	17	18	19	20	21	22	23	24	25	26
fraction	ladder	rec. (His)6-PCNA	cyto.	chr. unbd.	chr. bd.	cyto.	chr. unbd.	chr. bd.	cyto.	chr. unbd.	chr. bd.	cyto.	chr. unbd.	chr. bd.	cyto.	chr. unbd.	chr. bd.	cyto.	chr. unbd.	chr. bd.	cyto.	chr. unbd.	chr. bd.	cyto.	chr. unbd.	chr. bd.
inhibitor			**untreat. (DMSO)**			**erlotinib**			**gefitinib**			**lapatinib**			**imatinib**			**dasatinib**			**mastinib**			**LY294002**		
fraction	ladder	rec. (His)6-PCNA	cyto.	chr. unbd.	chr. bd.	cyto.	chr. unbd.	chr. bd.	cyto.	chr. unbd.	chr. bd.	cyto.	chr. unbd.	chr. bd.	cyto.	chr. unbd.	chr. bd.	cyto.	chr. unbd.	chr. bd.						
inhibitor			**U0126**			**SP600125**			**cherlerythrine chloride**			**NU7441**			**AZD2281**			**EGF stimulated**								

Both gels were run simultaneously at 150V for 2 hours using 1X MES running buffer (BioRad). Once the loading dye readed the bottom of the gel, the gels were removed from the plastic holding cases and put into deionized water until ready for Western blot transfer assembly.

Western Blot Transfer and Probing

Western blot transfer was performed immediately as per manufacturer's instructions (BioRad). Low fluorescence PVDF membrane (Immobilon-FL) was used in the transfer as well as 1X Tris-glycine transfer buffer containing 20% methanol. The transfer was performed at 100V (maximum current) for 30 minutes at 4°C (in cold room). An ice pack was also used to cool down the heat transferred into the transfer buffer.

Table 2.4

	antibody used	antibody supplier	concentration
primary	pY211-specific PCNA rabbit polyclonal antibody	Novus Biologics, cat no: NB100-598611; lot no: 9-1 (0.1uL)	1:1000
	PC10 total PCNA mouse monoclonal antibody	Santa Cruz Biotechnology, cat no: sc-56, lot no: I3010 (200ug/mL)	1:1000
secondary	mouse-anti-rabbit, FITC labeled antibody	Santa Cruz Biotechnology, cat no: sc-2359, lot no: D2211 (200ug/0.5mL)	1:1000
	goat-anti-mouse, FITC labeled antibody	Santa Cruz Biotechnology, cat no: sc-2010, lot no: L1410 (200ug/0.5mL)	1:1000

The Western blot was probed for the presence of pY211-PCNA (Novus Biologics) and total PCNA (Santa Cruz Biotechnology). It is essential to probe for pY211 first prior to stripping and re-probing for total PCNA.

The protocol for probing the blots is as follows:

1. Rehydrate the membrane in 1X TBS for 10 minutes prior to addition of blocking buffer (1X TBS in 1% BSA) for 1 hour.
2. After 1 hour, add in a 1:1000 dilution of primary antibody (see table above) and allow it to incubate for 2 hours at room temperature on an orbital mixer (rpm: 100).
3. After the 2 hour incubation, wash the blot three times (5 minutes each) with 1X TBS containing 0.5% Tween 20.
4. Add in a 1:1000 dilution of secondary antibody (see table above) and allow it to incubate for 1 hour at room temperature (dark) on an orbital mixer (rpm: 100).

5. After the 1 hour incubation, wash the blot three times (5 minutes each) with 1X TBS containing 0.5% Tween 20.
6. Image the membrane on a Typhoon Trio+ fluorescence scanner (GE Healthcare) at an excitation of 485nm (blue laser) and emissions collected at 526nm (fluorescein filter). Scanning was performed with pixel size of 100u and under normal sensitivity.
7. Images were processed through ImageQuant v.7. Individual pixel fluorescence intensities were exported into Excel for data analysis.
8. Blot was stripped in a solution of 500mM Tris HCl (pH 6.8), 10% SDS, and 150mM betamercaptoethanol for 30 minutes at 60°C.
9. After stripping, the blot was washed thoroughly with 1X TBS three times (5 minutes each), and then blocked (see step 2).

Images and Data Analysis

All images were visualized in QualityOne software (BioRad) and images exported as PNG files. Banding due to pY211-PCNA and total PCNA are shown below. Full blot images are located in ancillary data. The next page shows the images of the Western blots.

A similar blot as above was performed but using 50ug protein/well to try to enhance the signal of the pY211-PCNA protein band. This blot was used for data analysis. There are a lot of interesting observations that can be made with these blots. (1) The first was that the chromatin-bound fraction did not have significant amounts of PCNA and pY211-PCNA. It is wondering whether the strange banding at 15 and 6kDa molecular weight corresponds to PCNA degradation. (2) There is definitely a decrease in pY211 levels (compared to untreated) upon kinase inhibition. Further analysis will need to determine if the decrease is due to changes in total PCNA levels. (3) There are multiple bands that appear with the total PCNA lanes (especially in chromatin bound fractions). Are these bands due to other modifications such as ubiquitination or sumoylation?

All data analysis was performed in Microsoft Excel with the exported pixel fluorescence intensity values. Graphical representations and linear regression statistics were performed in GraphPad Prism. The method used for data analysis will be described in detail for enhanced understanding of this process. Automation would greatly help; however, positioning and lane assignments of the Western blots will need to become standardized. This process may be harder than just manually analyzing the data.

Image Analysis

The images generated were analyzed for total fluorescence intensity of the pixels that correspond to a specific protein band. The following steps were performed to generate number useful for comparisons and looking at the overall changes in pY211-PCNA status of PCNA upon kinase inhibition.

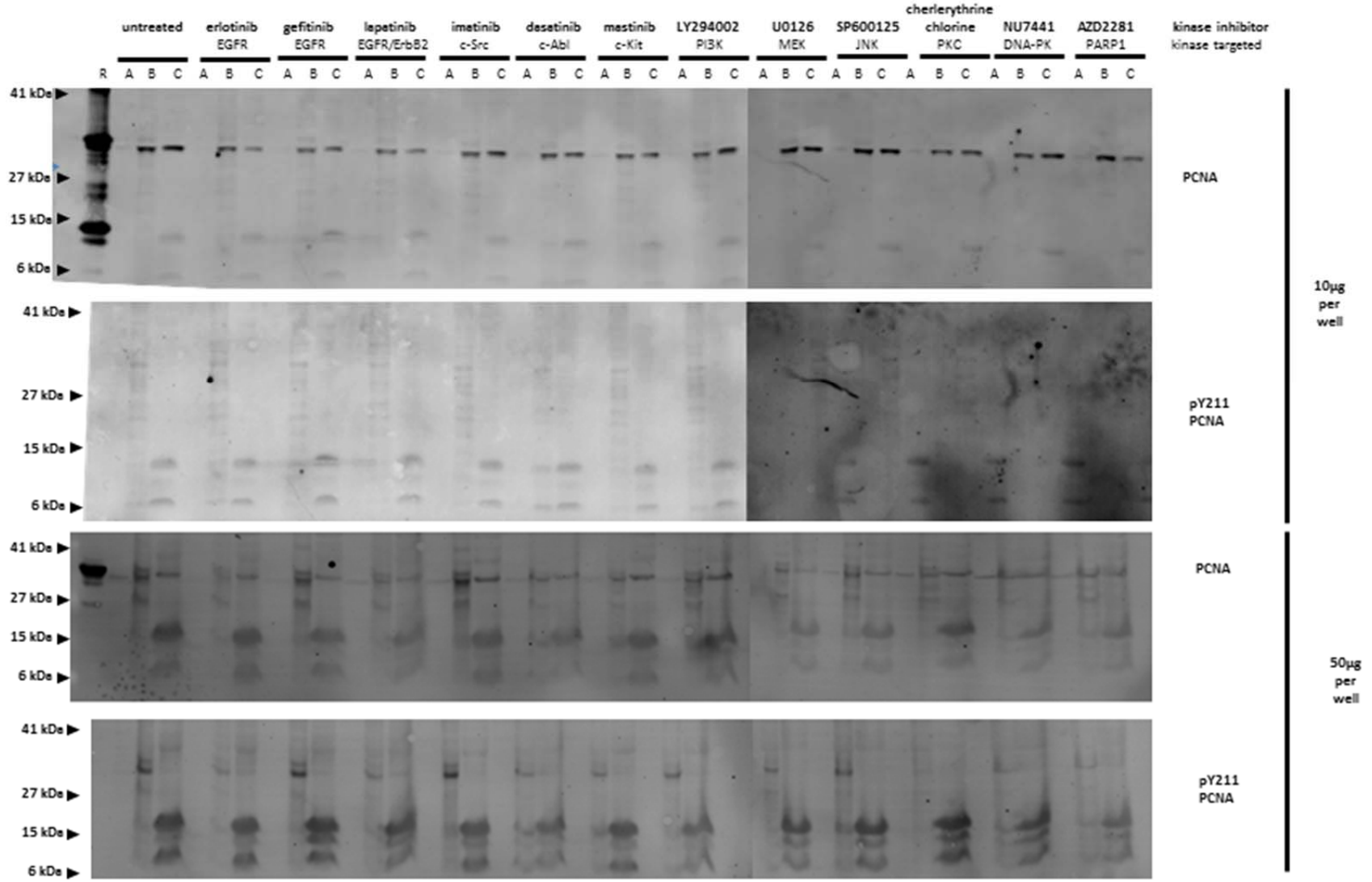

Effects on PCNA Phosphorylation upon Kinase Inhibition in MDA-MB-468 Breast Cancer Cells. 60-70% confluent cultures of MDA-MB-468 were serum starved for 24 hours prior to serum block removal and drug treatment (10µM) for an additional 24 hours. Cells were fractionated to afford cytoplasm (A), chromatin unbound nuclear (B), and chromatin bound nuclear (C) fractions. A total of 10µg of each lysate was loaded per lane. The blot was probed for the presence of pY211-PCNA and total PCNA using FITC-labeled secondary antibodies. Images were generated in QualityOne software (BioRad) after exciting the immunoblot at 485nm and collecting emissions at 526nm at 600W power and 100µ pixel resolution using a Typhoon Trio+ (GE Healthcare).

Key:
R recombinant PCNA
A cytoplasm fraction
B chromatin unbound nuclear fraction
C chromatin bound nuclear fraction

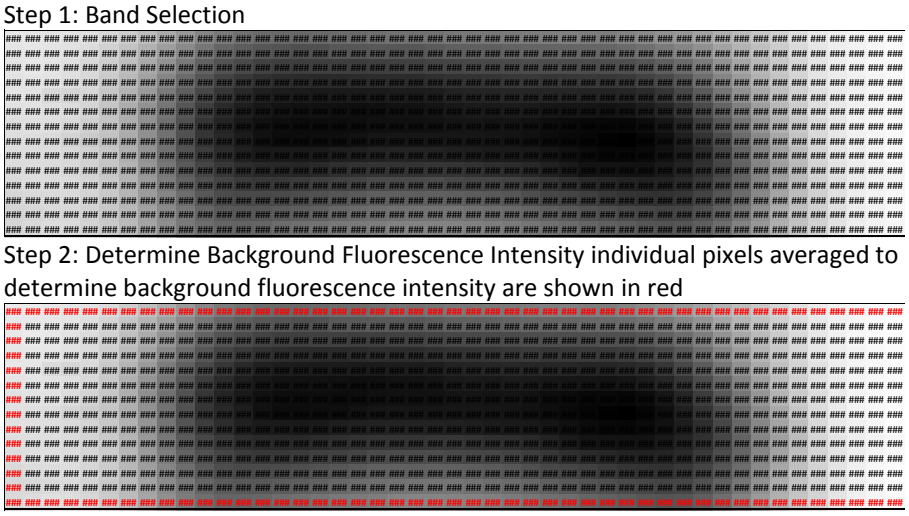

Figure 2.6: The basic data pipeline for reducing the imaging data for quantification of the Western blot assays.

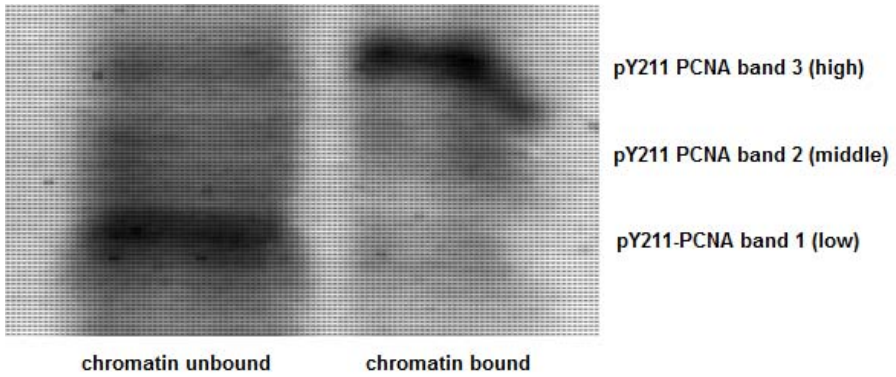

Figure 2.7: An example of the distinctions in the PCNA protein isoforms observed in the different nuclear fractions. Western blot images for the chromatin-bound vs chromatin-free fractions blotted for pY211-PCNA. The differences in protein structure promoting these different rates of migration are not known at this time.

Step 1: Identify a 14×50 pixel area that covers the entire band.

Step 2: Determine average background fluorescence intensity of the membrane around the band. To do this, average the fluorescence pixel intensity of all the pixels that perimeter the band (124 pixels total). An average and standard deviation is reported. The standard deviation is used to gauge the effectiveness of selecting the proper pixel range.

Step 3: The fluorescence intensity of each pixel was subtracted from individual pixel fluorescence intensity to afford a background subtracted band.

Step 4: The sum of all fluorescence intensities in the 14×50 area defined, after background subtraction was calculated. This value will be compared to the untreated to look at fold change in expression levels.

Step 5: Regression analysis was performed to identify the kinase inhibitors that demonstrated the most significant (and statistically and visually) change in pY211 levels. This subset of kinase inhibitors will be tested further for validation and more

The following page shows the data that was reduced. Upon the analysis, several bands were observed in the total and pY211-PCNA lanes. It is uncertain whether any of these additional bands are truly due to PCNA. This is one of the reasons why the pY211-PCNA antibody has to be followed by additional analyses. In the case of total PCNA blots, only the low and middle bands were observed. It is uncertain what the high band is and why it only occurs in the chromatin bound fraction. Is this non-specific binding?

Since the top band (high) does not correlate with any of the bands with total PCNA, the band was removed from analysis when trying to see if changes in pY211 status of PCNA are due to changes in total PCNA expression. To do this, the ratio of total band fluorescence was divided by that of the untreated band and graphically represented in GraphPad Prism. For the sake of simplicity, total nuclear content was determined instead of comparing chromatin bound and unbound individually.

MDA-MB-468 TNBC Cell Line Western Blot Analysis

			total PCNA (PC10 mAb)					pY211 - PCNA (pAb)				
	molecular		background		band	total	percentage	background		band	total	percentage
treatment	target	fraction	average	st. dev	sum	band sum	of untreated	average	st. dev	sum	band sum	of untreated
untreated	--	chromatin unbound (high)	7153	526	141716	557003	1.000	6247	262	115494	420500	1.000
		chromatin unbound (low)	7384	533	170383			6684	715	305006		
		chromatin bound (high)	--	--	--			6563	630	150958		
		chromatin bound (low)	6937	198	244904			--	--	--		
erlotinib	EGFR	chromatin unbound (high)	6667	435	163034	546913	0.982	5775	141	23698	253348	0.602
		chromatin unbound (middle)	--	--	--			*5899*	*201*	*29840*		
		chromatin unbound (low)	6929	599	232496			5901	257	117611		
		chromatin bound (high)	--	--	--			6108	261	114148		
		chromatin bound (middle)	--	--	--			*5986*	*199*	*66172*		
		chromatin bound (low)	6467	142	151383			5938	179	82199		
gefitinib	EGFR	chromatin unbound (high)	6421	307	93539	330069	0.593	6318	475	172553	594697	1.414
		chromatin unbound (low)	6407	324	102585			6573	718	422144		
		chromatin bound (high)	--	--	--			6146	188	85012		
		chromatin bound (low)	6463	235	133945			--	--	--		
lapatinib	EGFR/ErbB2	chromatin unbound (high)	6384	289	84591	321689	0.578	5888	174	40362	282319	0.671
		chromatin unbound (middle)	--	--	--			*5923*	*225*	*43476*		
		chromatin unbound (low)	6427	296	121401			6018	333	155869		
		chromatin bound (high)	--	--	--			6062	204	75703		
		chromatin bound (low)	6500	206	115697			5977	206	86088		
imatinib	c-Src	chromatin unbound (high)	6816	520	174576	833733	1.497	6167	527	171297	583686	1.388
		chromatin unbound (low)	7228	774	289753			6450	834	412389		
		chromatin bound (high)	--	--	--			5710	94	70654		
		chromatin bound (low)	6684	197	369404			--	--	--		
dasatinib	c-Abl	chromatin unbound (high)	--	--	--	266038	0.478	--	--	--	162111	0.386
		chromatin unbound (low)	6630	264	140191			6048	331	147929		
		chromatin bound (high)	--	--	--			--	--	--		
		chromatin bound (low)	6486	164	125847			5957	123	14182		
mastinib	c-Kit	chromatin unbound (high)	--	--	--	404511	0.726	5711	86	30875	222267	0.529
		chromatin unboud (middle)						5884	210	46380		
		chromatin unbound (low)	6485	228	137454			5913	265	177447		
		chromatin bound (high)						5770	127	90181		
		chromatin bound (middle)						5706	115	38082		
		chromatin bound (low)	6536	209	267057			5700	110	44820		
LY294002	PI3K	chromatin unbound (high)	6612	360	75235	484855	0.870	5675	221	53247	294466	0.700
		chromatin unbound (low)	6851	411	175749			5886	403	241219		
		chromatin bound (high)	--	--	--			5689	270	54684		
		chromatin bound (low)	7061	376	233871			--	--	--		
U0126	MEK	chromatin unbound (high)	6237	215	34871	253568	0.455	6082	115	16834	175645	0.418
		chromatin unbound (middle)	--	--	--			6168	156	22564		
		chromatin unbound (low)	6353	227	117428			6255	208	158811		
		chromatin bound (high)	--	--	--			6018	171	9750		
		chromatin bound (low)	5998	142	101269			--	--	--		
SP600125	JNK	chromatin unbound (high)	6390	346	84274	420087	0.754	6365	243	47356	287077	0.683
		chromatin unbound (low)	6624	467	176130			6603	513	239721		
		chromatin bound (high)	--	--	--			6265	103	34025		
		chromatin bound (low)	5437	154	159683			--	--	--		
cherlerythrine chloride	PKC	chromatin unbound (high)	6709	237	62307	426167	0.765	6241	156	59790	129552	0.308
		chromatin unbound (low)	2836	247	148518			6339	142	53976		
		chromatin bound	6932	212	215342			6181	97	15786		
NU7441	DNA-PK	chromatin unbound (high)	--	--	--	284947	0.512	--	--	--	96039	0.228
		chromatin unbound (low)	6637	258	136667			6452	277	96039		
		chromatin bound (high)						6260	164	31774		
		chromatin bound (low)	6619	217	148280			--	--	--		
AZD2281	PARP-1	chromatin unbound (high)	6191	180	34214	287125	0.515				147886	0.352
		chromatin unbound (low)	6340	190	130284			5823	239	109672		
		chromatin bound (low)	6412	227	122627			5674	78	38214		

Appendix 3: Synthesis of Peptides, Peptoids and Conjugates

PCNA-derived peptides: Synthetic peptides will be used in the confirmation of whether or not nuclear tyrosine kinases accept a PCNA-specific sequence that includes the amino acid residue tyrosine 211 (Y211). Relative amounts of phosphorylation of the difference peptide sequences by various tyrosine kinases will be quantified using capillary electrophoresis (equipped with a photodiode array) and this information will be used to argue that nuclear tyrosine kinases directly interact with and phosphorylate PCNA.

Three peptides derived from the twelve amino acid residues surrounding PCNA Y211 have been synthesized as well as a randomized sequence to serve as a control. The randomized sequence, henceforth referred to as "scrambled," contains the same residues as the PCNA derived sequences, but in a randomized order.[5] The peptides, written N-terminal to C-terminal from left to right, are as follows:

PCNA Y211:	TFALRYLNFFTK	anticipated m/z 1520.8260, observed m/z 1520.7942
PCNA Y211F:	TFALRFLNFFTK	anticipated m/z 1504.8311, observed m/z 1504.7515
PCNA pY211:	TFALRpYLNFFTK	anticipated m/z 1600.7923, observed m/z 1599.8541
PCNA scrambled:	FLFTNKLFRTAF	anticipated m/z 1504.8311, observed m/z 1503.8320

The PCNA Y211F peptide is used as a negative control—tyrosine being replaced with phenylalanine should not allow for phosphorylation. PCNA pY211 is used as a positive control as the tyrosine residue remains phosphorylated.

Nuclear-targeted peptides and peptoids: Several prior studies have shown that molecules can be targeted to the nucleus of cells through the use of various nuclear targeting sequences, often consisting of, but not limited to, short peptide sequences derived from viruses such as Human Immunodeficiency Virus 1 or Simian vacuolating virus 40.[6–10] These peptides can be attached to other molecules that range in size from small, drug-like molecules (MW<500) to mesoporous silica nanoparticles that act as high-payload drug delivery transporters; this has been shown to increase the efficiency of drug delivery and improves the respective desired effect.[11–13] Additionally, various forms of peptides and peptoids have been seen to act as cell penetrating sequences (see figure below), increasing the cellular uptake of the molecule, thereby increasing its cytoplasmic and/or nuclear concentrations.[12,14–19] These strategies for drug targeting can be used to good effect, and when combined can greatly increase the efficiency with which a drug is taken up into the cell, ultimately improving its potency. Here, nuclear delivery of known experimental therapeutics is explored to assess if nuclear tyrosine kinase inhibition is a useful pharmacologic endpoint in breast cancer models; additionally, this strategy is used to test whether targeting nuclear tyrosine kinases with tyrosine kinase inhibitors can downregulate levels of Y211 phosphorylated PCNA.

Several peptoids (poly N-alkyl substituted glycines) have been synthesized that are comprised of seven or nine consecutive amino acid analogues representing lysine (peptoid nomenclature: NLys). These ‘lysine’ peptoids are N-terminally conjugated, separated by a 6-aminohexanoic acid linker (Ahx), to a chemically modified form of the EGFR inhibitor gefitinib (trade name Iressa; labeled “Gef”), 5-carboxyfluorescein (5-FAM) or simply 6-aminohexanoic acid which serves as a control. A ‘nuclear targeted’ peptoid contains a seven amino acid peptide sequence derived from the simian virus 40 large T antigen (SV40).[18] The SV40 sequence is separated from the peptoid and N-terminal conjugate by 6-aminohexanoic acid linkers. Peptides/peptoids were fluorescently labeled with 5-FAM to examine their propensity for cellular uptake and subcellular localization. A fluorescently labeled sequence derived from the HIV TAT peptide[5] was used as a benchmark for cellular uptake and delivery.

The peptides/peptoids, written N-terminal to C-terminal from left to right, are as follows (residues in brackets indicate peptoids):

Peptides and Peptoids Synthesized for Nuclear localization of Protein Kinase Inhibitor

TAT	CGRKKRRQRRRG
TAT-PCNA scrambled	Ahx- CGRKKRRQRRRG-FLFTNKLFRTAF
TAT-PCNA-Y211F	Ahx-CGRKKRRQRRRG- TFALRFLNFFTK
(5-FAM)-TAT-Y211F	5-FAM-Ahx-CGRKKRRQRRRG- TFALRFLNFFTK
(5-FAM)-TAT	5-FAM-Ahx-CGRKKRRQRRRG
$NLys_9$:	Ahx-[KKKKKKKKK]
SV40-$NLys_9$:	Ahx-PKKKRKV-Ahx-[KKKKKKKKK]
(5-FAM)-$NLys_7$:	(5-FAM)-Ahx-[KKKKKKK]
(5-FAM)-$NLys_9$:	(5-FAM)-Ahx-[KKKKKKKKK]
(5-FAM)-SV40-$NLys_9$:	(5-FAM)-Ahx-PKKKRKV-Ahx-[KKKKKKKKK]
(5-FAM)-TAT:	(5-FAM)-Ahx-CGRKKRRQRRRG

The peptides used in this study have been synthesized by two methods: manual solid phase synthesis and automated synthesis using an Intavis peptide synthesizer. Peptoids and peptide-peptoid conjugates were synthesized using manual solid phase synthesis. Identity and amino acid order are confirmed using MALDI and TOF-TOF mass spectrometry.

Solid Phase Peptide Synthesis

0.100 mmol of Rink Amide Tentagel Resin (substitution value: 0.71 mmol eq/g resin) is weighed and transferred to a peptide reaction vessel. 5mL of dimethylformamide (DMF) is added to the resin and the resin is allowed to swell for 30 minutes. The DMF is removed, and 3mL of a 20% piperidine in DMF solution is added to the reaction vessel containing the resin; the resin is allowed to incubate at room temperature for 30 minutes with shaking in order to deprotect the resin. After the 30 minute incubation, the resin is washed six times with DMF and then three times with dichloromethane (DCM). Deprotection is confirmed via a Ninhydrin test (Kaiser's test; described below). A solution of 2.1 ml 0.45M O-(1H-6-Chlorobenzotriazole-1-yl)-1,1,3,3-tetramethyluronium hexafluorophosphate (HCTU) in DMF, 435µl 2M diisopropylethylamine (DIEA), and 1 mmol (10 equivalents) of the respective Fmoc-protected amino acid is added to the resin, and the resin is incubated at room temperature with shaking for one hour. After one hour, the resin is washed six times with DMF and three times with DCM. Residue coupling is confirmed via a Ninhydrin test. The de-protection and coupling steps are repeated until the entire peptide has been synthesized. After the final amino acid residue has been de-protected and the resin washed as before, a solution of TFA/H_2O/TIS (95:2.5:2.5) is added to the resin with incubation at room temperature for four hours. At that time, the resin is filtered from the supernatant and the peptide is precipitated into diethyl ether. The peptide is then stored at -20°C.

In preparation for mass spec analysis and peptide purification, the diethyl ether is evaporated and the remaining residue is dissolved in acetonitrile/water (1:1).

Solid Phase Submonomer Peptoid Synthesis[20]

0.100 mmol of H-Rink Amide ChemMatrix resin (substitution value: 0.25 mmol eq/g resin) is weighed and transferred to a peptide reaction vessel. 5mL of dimethylformamide (DMF) is added to the resin and the resin is allowed to swell for 30 minutes. The DMF is removed, and 3mL of a 20% piperidine in DMF solution is added to the reaction vessel containing the resin; the resin is allowed to incubate at room temperature for 30 minutes with shaking in order to deprotect the resin. After the 30 minute incubation, the resin is washed six times with DMF and then three times with dichloromethane (DCM). Deprotection is confirmed via a Ninhydrin test (Kaiser's test; described below). A solution of 2.5 ml of 1M bromoacetic acid in DMF and 382 µl N,N′-diisopropylcarbodiimide is added to the resin, and the resin is incubated at 37°C with shaking for 40 minutes. At that time, the resin is washed six times with DMF and three times with DCM. Coupling is confirmed via a Ninhydrin test. Then, a solution of 1M tert-butyl (4-aminobutyl)carbamate in DMF is added to the resin, and the

resin is incubated at 37°C with shaking for two hours. At that time, the resin is washed six times with DMF and three times with DCM. Subsequent couplings are confirmed via a chloranil test (described below). Bromoacetic acid and tert-butyl (4-aminobutyl)carbamate couplings are alternated to produce the peptoid of desired length. In addition to the SV40 amino acids, 6-aminohexanoic acid, modified gefitinib and 5-carboxyfluorescein are coupled using the conditions listed under solid phase peptide synthesis (along with confirmations via Ninhydrin tests). After the final reagent has been coupled and the resin washed as before, a solution of TFA/H_2O/TIS (95:2.5:2.5) is added to the resin with incubation at room temperature for three hours. At that time, the resin is filtered from the supernatant, and the TFA solution is evaporated with gently blowing air. The residue that remains is redissolved into ACN/H_2O (60:40), frozen at -80°C and lyophilized overnight. Dissolution in ACN/H_2O, freezing and lyophilization is repeated once more, and the remaining peptoid is stored at -20°C in preparation for mass spec analysis and peptoid purification.

Synthesis of Peptide and Peptoid Conjugates with Gefitinib

Peptoids or peptoid-peptide conjugates containing a deprotected 6-aminohexanoic acid primary amine were coupled to the carboxylic acid functionality of piperazinyl gefitinib using a protocol described in **Appendix 4**. The resulting conjugate molecules consisted of a cell penetrating sequence (shown in red below) and/or a nuclear localization sequence separated from the N-terminally located piperazinyl gefitinib by a 6-aminohexanoic acid linker. This linker region would ideally project out of the gefitinib binding pocket on EGFR towards solution, as is depicted below.

Gef-TAT Gef-hexyl-CGRKKRRQRRRG

Gef-$NLys_9$: Gef-Ahx-[KKKKKKKKK]

Gef-SV40-$NLys_9$: Gef-Ahx-PKKKRKV-Ahx-[KKKKKKKKK]

Synthesis of First Generation TAT-Peptide-Gefitinib Conjugate for Nuclear Localization: Previously, versions of a Tat peptide have been demonstrated to localize proteins and other biomolecules to the nucleus. The Tat peptide, **8** was synthesized by solid phase peptide synthesis with Fmoc-*N*-protected amino acids on Rink Amide AM resin using an Intavis MultiPep automated peptide synthesizer. Fmoc-azidohomoalanine was conjugated to part of the immobilized Tat peptide to yield a peptide capable of undergoing a [3+2] cycloaddition reaction.

Two strategies for conjugation of the Tat peptide and gefitinib were pursued. In the first and more direct method (Method 1), the propargyl-gefitinib was coupled with the immobilized azido-Tat peptide, **9** via a copper (I) catalyzed [3+2] cycloaddition for 16 hours at room temperature in the dark. The click product was removed from the resin using a 95%/2.5%/2.5% solution of TFA/triisopropylsilane/water for 4 hours and then precipitated into iced cold diethyl ether. These reactions were did not yield successfully coupled product. An alternative approach was to first introduce 6-azidohexanoic acid, **10** in a copper(I) catalyzed [3+2] cycloaddition reaction with propargyl-gefitinib. After HPLC purification and MALDI-TOF analyses of the product, **11**, a second step proceeded via HBTU/DIPEA coupling reaction with the immobilized Tat peptide.

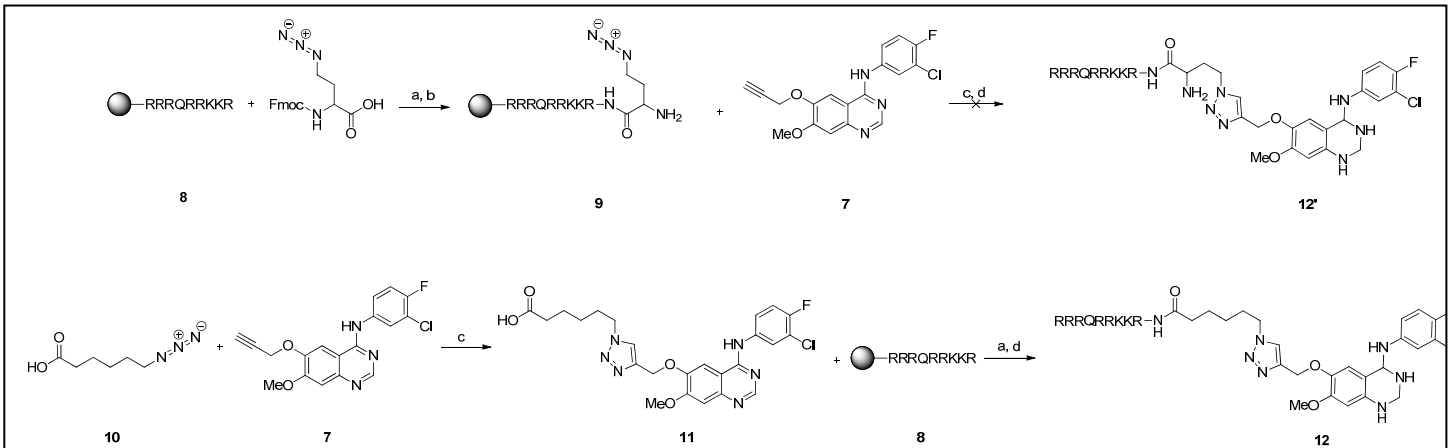

Scheme 2. Syntheses of Tat-Gefitinib Conjugate. Conditions: (a) HBTU, DIPEA, DMF, 1 h; (b) 20% piperidine, DMF, 20 min; (c) CuI, ascorbic acid, DIPEA, DMF, pyr, 16 h, dark; (d) trifluoroacetic acid, triisopropylsilane, water (95%/2.5%/2.5%), 4 h

After cleavage of the product from the resin using 95%/2.5%/2.5% solution of TFA/triisopropylsilane/water, HPLC purification and MALDI-TOF analyses confirmed the final product, **12** albeit in 3% overall yield based upon propagyl-gefitinib.

Methods

Resin-Tat Peptide (**8**) Solid phase peptide synthesis was performed on Rink Amide AM resin (Novabiochem, 100μmol, 0.71mmol eq/g resin). Fmoc-protected amino acids and resin were deprotected using 20% piperidine in DMF for 20 min. Fmoc-protected amino acids (5 equiv.) were coupled under standard peptide synthesis conditions [O-benzotriazole-N,N,N',N'-tetramethyl-uronium hexafluorophosphate (5 equiv), DIPEA (10 equiv.)] for 1 h at room temperature. After coupling and deprotection steps, the resin was washed with DMF (6x). Reactions were monitored through a ninhydrin (Kasier's) test. To determine purity and validate synthesis of peptide, a small fraction of resin was removed and cleaved using 95:2.5:2.5 trifluoroacetic acid/triisopropylsilane/water cocktail for 4 hours at room temperature. MALDI-TOF: predicted 1338.87, observed 1338.79 (M^+).

Resin-Azido-Tat Peptide (**9**) Fmoc-azidohomoalanine (BaChem, 1.1 equiv.) was dissolved in 2.5mL of a DMF solution containing *O*-benzotriazole-*N,N,N',N'*-tetramethyl-uronium hexafluorophosphate (5 equiv.), DIPEA (10 equiv.), and **8** for 1 hour at room temperature. Resin was washed with DMF (6x) and deprotected with 20% piperidine in DMF (20 min). Coupling and deprotection reactions were monitored by ninhydrin (Kaiser's) test. Resin was dried for 30 minutes on vacuum and stored at -20°C until needed. A small fraction of resin was removed and cleaved using 95:2.5:2.5 trifluoroacetic acid/triisopropylsilane/water cocktail for 4 hours at room temperature. MALDI-TOF: predicted 1466.1, not verified.

Gefitinib-Linked Tat Peptide, Method 1 (**12'**) Propargylated gefitinib, **7** (10μmol), was added to a 7:3 solution of DMF/pyridine containing **2** (1 equiv.), copper iodide (2 equiv.), ascorbic acid (1 equiv.), and DIPEA (2 equiv.) and allowed to incubate while shaking for 16 hours, dark. Resin was washed with DMF (6x) and dried for 30 minutes on vacuum. Resin immobilized **12** was cleaved in trifluoroacetic acid/triisopropylsilane/water (95%/2.5%/2.5%) for 4 hours at room temperature. Resin was removed from the solution and added dropwise into cold, diethyl ether. The precipitate was centrifuged at 1,000rcf for 5 minutes at 4°C. Excess diethyl ether was removed and the peptide was purified by HPLC immediately under standard peptide purification gradient (5-100% acetonitrile in 0.1% trifluoroacetic acid in water containing 0.1% trifluoroacetic acid over 30 minutes) with a Zorbax C18 semi-preparative C_{18} column. HPLC trace at 215nm and 330nm indicated no coupling. MALDI-TOF: predicted 1823.1, not verified.

Aminohexanoic-Linked Gefitinib (**11**) 6-azido-hexanoic acid (BaChem, 100μmol), **3** was dissolved in 1mL of DMF containing 10 μmol of **2**, 2 equiv. copper (I) iodide, 1 equiv. ascorbic acid, and 2 equiv. of diisopropylethylamine. The resulting solution was sonicated and allowed to incubate at room temperature for 16 hours under Ar, dark conditions. Purity: 87.2%. Percent Yield: 68%. MALDI-TOF: predicted: 514.9, observed: 515.2.

Gefitinib-Linked Tat Peptide, Method 2 (**12**) 6-aminohexanoic-linked gefitinib, **11** (10μmol) was dissolved in 1mL of DMF containing *O*-benzotriazole-*N,N,N',N'*-tetramethyl-uronium hexafluorophosphate (1 equiv.), DIPEA (2 equiv.), and **8** for 4 hours at room temperature. Resin was washed with DMF (6x) and deprotected with 20% piperidine in DMF (20 min). Coupling reaction was monitored by ninhydrin (Kaiser's) test. Resin was dried for 30 minutes on vacuum and stored at -20°C until needed. The material was cleaved from resin in trifluoroacetic acid/triisopropylsilane/water (95%/2.5%/2.5%) for 4 hours at room temperature. Resin was removed from the solution and added dropwise to cold, diethyl ether. The precipitate was centrifuged at 1,000rcf for 5 minutes at 4°C. Excess diethyl ether was removed and the peptide was purified by HPLC immediately under standard peptide purification gradient (5-100% acetonitrile in 0.1% trifluoroacetic acid in water containing 0.1% trifluoroacetic acid over 30 minutes) with a Zorbax C18 semi-preparative C_{18} column. Purity: 64%. Percent Yield: 3%. MALDI-TOF: predicted: 1823.1, observed: 1834.9807 (MH^+).

Solid Phase Synthesis of Peptoid-Peptide-Gefitinib Conjugates

The peptoid portion of the molecule is synthesized as described above using the submonomer method. After the full peptoid has been synthesized, 6-aminohexanoic acid is coupled at the N-terminus using the standard peptide amino acid coupling procedure. In the case of the SV40-conjugated molecules, the SV40 peptide sequence is also synthesized according to the standard peptide amino acid coupling procedure, with 6-aminohexanoic acid again being coupled at the N-terminus after completion of the SV40 sequence. After Fmoc deprotection of the N-terminal 6-aminohexanoic acid, and dividing the resin into two separate portions, a solution of 63 mg (0.125 mmol) piperazinyl gefitinib, 51 mg (0.1249 mmol) HCTU and 32 mg (0.25 mmol) DIEA, dissolved up to 2.5 ml DMF, is added to one portion of the resin, allowing the resin to incubate overnight at room temperature on an orbital shaker. Coupling is confirmed using a ninhydrin test, and the conjugate molecule is cleaved from resin and HPLC purified using the procedures described above.

Ninhydrin (Kaiser's) Test

Solutions used:

- 5g ninhydrin in 100ml ethanol
- 80g phenol in 20ml ethanol
- .02 mM potassium cyanide in pyridine

To a small amount of washed resin is added three drops of each of the three solutions used in the test. The resin is placed at 100°C for five minutes—at that time, a dark blue solution indicates the presence of a primary amine (deprotected residue); otherwise, the solution remains yellow.

Chloranil Test

Solutions used:

- 2% chloranil in DMF
- 2% acetaldehyde in DMF

To a small amount of washed resin is added 20 µl of each solution. The resin is placed at 100°C for five minutes—at that time, a dark blue solution indicates the presence of a primary amine, a blue/red solution indicates the presence of a secondary amine, and no color change indicates the presence of a tertiary amine.

Peptide/Peptoid Purification

The peptides/peptoids are purified on a reverse phase semi-prep HPLC column using a gradient of acetonitrile with 0.1% TFA / water with 0.1% TFA from (5:95) to (100:0) over the course of 30 minutes. The flow-through is collected and lyophilized to give the purified sample.

Appendix 4. Synthesis of Gefitinib Analogs

The synthesis of alkynyl gefitinib was performed to produce a moiety in which a nuclear targeting moiety can be attached for delivery of the gefitinib moiety to the nucleus. The synthetic steps to alkynyl gefitinib, **7, 9, 11-13** have been completed (Schemes 1 and 2). These tyrosine kinase inhibitor analogs were used in the development and testing of conjugates that are targeted toward nuclear kinases. The ultimate applications are for improved options in treatment of patients with refractory and/or drug resistant breast cancers.

Scheme 4.1: Synthesis of Alkynyl Gefitinib.

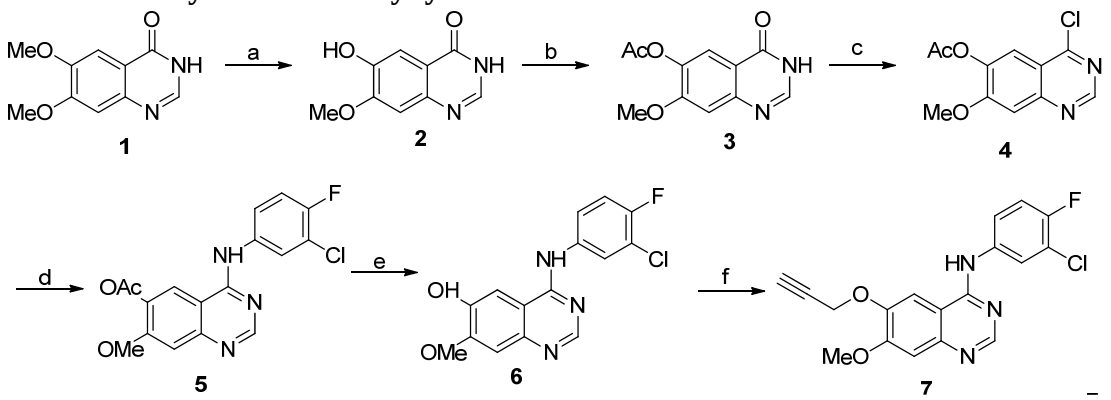

Conditions: (a) methanesulfonic acid, L-methionine, 110-120^{o}C, 6 h, 88%; (b) Ac_2O, pyridine, DMAP, 80%; (c) $POCl_3$, DEA; (d) 3-chloro-4-fluorophenylamine, isopropanol, 88% for 2 steps; (e) LiOH/MeOH-H_2O, 85%; (f) propargyl bromide, K_2CO_3, DMF, 79%.

Scheme 4.2: Synthesis of Alternative Water Soluble Gefitinib

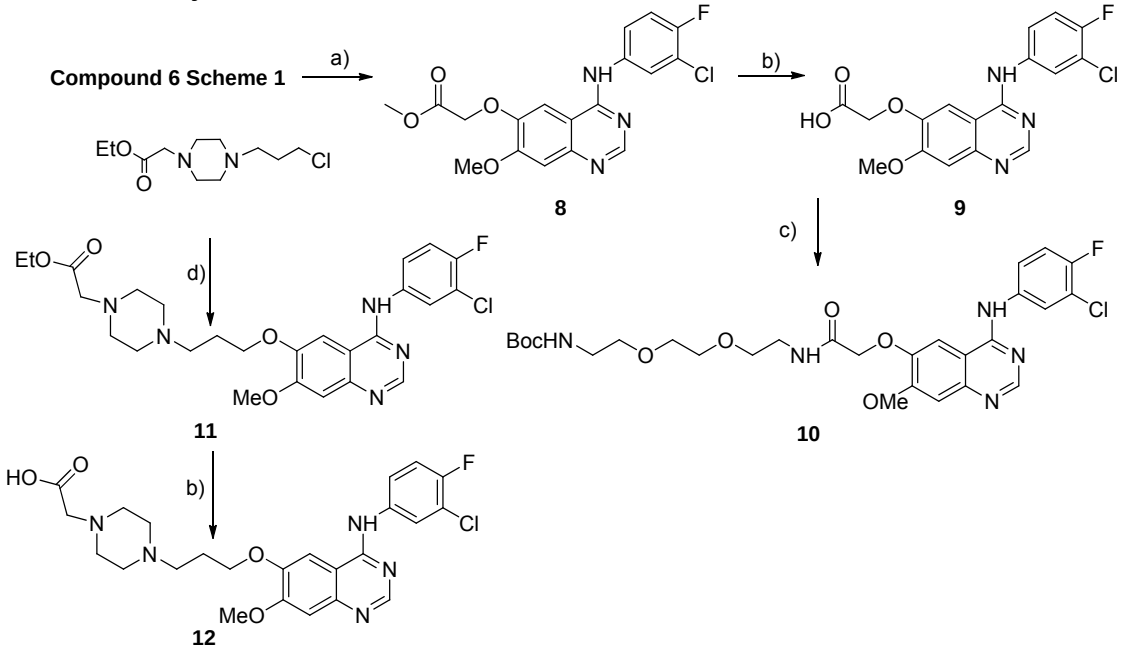

Conditions: a) Methyl bromoacetate, K_2CO_3, DMF, 96 %; b) LiOH 0.2 M, i-PrOH/H_2O = 1.2/1, 23 oC, 94 %; c) 2-(2-(2-t-Butoxycarbonylaminoethoxy)ethoxy)-ethylamine, HBTU, DIPEA, DMF, 99 %; d) NaI, K_2CO_3, DMF, 60 oC, 92 %.

Synthesis of Piperazinyl Gefitinib-tagged Peptoid/Peptides: A modified form of the commercially available EGFR inhibitor gefitinib is used in an effort to enhance the efficacy of its apoptosis-inducing effect. Targeting the activity of nuclear-located EGFR may decrease the levels of phosphorylated PCNA, thereby enhancing DNA damage through the downregulation of PCNA's DNA damage response. This is based on previous work that suggests EGFR interacts directly with PCNA and phosphorylates it.[1,5,21] The morpholine functional group on commercial gefitinib was replaced with a piperazinyl acetate functionality that allows for the attachment of

amines using basic peptide coupling reagents such as HCTU and DIC,[22,23] while attempting to minimally impact the chemical divergence of the core drug molecule. Piperazinyl gefitinib was synthesized in-house using the synthetic scheme shown below:

Experimental

Unless stated otherwise, all reagents and solvents were used as received from commercial suppliers. Unless stated otherwise, all reactions were conducted in dried, anhydrous solvents. Filtration was generally performed through a pad of Celite. TLC analyses were performed on Merck aluminum-backed F254 silica gel plates. Flash chromatography was performed using silica gel (ICN 60 Å silica gel, 32-63 μ) and samples were applied using CH_2Cl_2. NMR spectra were measured at the frequencies indicated on a 300 MHz Bruker instrument. All ^1H chemical shifts (δ) are relative to residual protic solvent ($CHCl_3$: δ 7.26, DMSO-d_6: δ 2.50, CD_3OD: δ 3.31 ppm), and all ^{13}C chemical shifts (δ) are relative to the solvent ($CDCl_3$: δ 77.23, DMSO-d_6: δ 39.52, CD_3OD: δ 49.00 ppm).

6-Hydroxy-7-methoxyquinazolin-4(3H)-one (**2**)

A mixture of 6,7-dimethoxyquinazolin-4(3H)-one (3.0 g, 14.5 mmol) and L-methionine (2.6 g, 17.2 mmol) was dissolved in methanesulfonic acid (20.5 mL) and heated to 110-120 ^oC for 6 h. Heating the reaction at 120 ^oC or above resulted in the production of 2' isomer. When the reaction was complete, the mixture was poured into the crushed ice. Then NaOH (40% water solution) was added slowly (pH~7) resulting in precipitation of a white deposit. This product was collected by filtration, washed with water, cold ethanol, diethyl ether and dried in the air to afford the product (2.45 g, 88%) which was used without further purification.

^1H-NMR (300 MHz, DMSO-d_6): δ = 11.94 (s, I H), 9.80 (s, I H), 7.91 (s, I H), 7.36 (s, I H), 7.09 (s, I H), 3.90 (s, 3 H)

7-Methoxy-4-oxo-3,4-dihydroquinazolin-6-yl acetate (**3**)

A suspension of 6-hydroxy-7-methoxyquinazolin-4(*3H*)-one (2, 2.4 g, 12.5 mmol) in acetic anhydride (15 mL), pyridine (3.0 mL) and *N,N*-dimethyl-4-aminopyridine (15 mg) was stirred and heated to 100 -110 °C under Ar atmosphere for 4 h. The mixture was then poured into the crushed ice, and stirred vigorously for half an hour. The resulting white deposit was filtered, washed with water, cold EtOH, and Et_2O. The solid was further dried at 60 ^oC overnight to afford the product 3 (2.34 g, 80 %).

^1H-NMR (300 MHz, DMSO-d_6): δ = 12.21 (s, 1 H), 8.09 (s, 1 H), 7.75 (s, 1 H), 7.27 (s, 1 H), 3.91 (s, 3 H), 2.30 (s, 3 H)

4-Chloro-7-methoxyquinazolin-6-yl acetate (**4**)

To a solution of 7-methoxy-4-oxo-3,4-dihydroquinazolin-6-yl acetate (3, 468 mg, 2 mmol) and diisopropyl ethylamine (1.05 mL) in DCE (dichloroethane, 14 mL) was dropped phosphoryl chloride (0.28 mL). The whole mixture was immersed in a preheated oil bath (80 °C) and stirred at this temperature for 3 h. The reaction was monitored by TLC, the excess reagent and solvent were removed by rotary evaporation and under reduced pressure to afford the product **4**, which can be used directly for next step.

4-[(3-Chloro-4-fluorophenyl)amino]-7-methoxyquinazolin-6-yl acetate (**5**)

A solution of 4-chloro-7-methoxyquinazolin-6-yl acetate 4 (prepared above, 2 mmol) and 3-chloro-4-fluorophenylamine (320 mg, 2.2 mmol) in i-PrOH (5 mL) was stirred and heated to reflux under Ar atmosphere for 5 h. Reaction progress was monitored by TLC and starting materials were not detected after this time. The reaction mixture was cooled to room temperature and the obtained precipitate was filtered through a glass funnel, with i-PrOH and Et_2O and dried under reduced pressure to provide the product **5** (635 mg, 88 % for 2 steps) as an off-white powder.

^1H-NMR (300 MHz, DMSO-d_6): δ = 11.51 (s, br, 1 H), 8.94 (s, 1 H), 8.77 (s, 1 H), 8.01-8.09 (m, 1 H), 7.70-7.78 (m, 1 H), 7.48-7.55 (m, 2 H), 4.00 (s, 3 H), 2.38 (s, 3 H)

4-[(3-Chloro-4-fluorophenyl)amino]-7-methoxyquinazolin-6-ol (**6**)

The above 4-[(3-Chloro-4-fluorophenyl)amino]-7-methoxyquinazolin-6-yl acetate (5) (500 mg, 1.38 mmol) was dispersed in mixed solvent of methanol (35 mL) and H_2O (35 mL) at room temperature. Lithium hydroxide (109 mg, 4.6 mmol) was added and the mixture was stirred at room temperature for 0.5 h. When the reaction was complete as monitored by TLC, the mixture was neutralized by the addition of diluted acetic acid. The resultant precipitate was collected by filtration, washed with water, cold EtOH, and Et_2O, and dried under reduced pressure to give the product **6** (373 mg, 85 %).
^{1}H-NMR (300 MHz, DMSO-d_6): δ = 9.79 (s, 1 H), 9.47 (s, 1 H), 8.45 (s, 1 H), 8.13-8.20 (m, 1 H), 7.70-7.85 (m, 2 H), 7.38 (t, *J* = 10.2 Hz, 1 H), 7.19 (s, 1 H), 3.96 (s, 3 H)

4-(3'-Chloro-40-fluoroanilino)-6-(prop-2-ynyloxy)-7-methoxyquinazoline (**7**)

To a solution of 6 (80 mg, 0.25 mmol) in DMF (3 ml) were added propargylbromide (60 □l, 0.56 mmol) and K_2CO_3 (42mg, 0.30 mmol) and the mixture was stirred for 12 h at room temperature and monitored by TLC. The reaction was quenched with water and the mixture was extracted with ethyl acetate, dried over anhydrous Na_2SO4, and concentrated. Purification by column chromatography on silica gel with dichloromethane/methanol (100/1 – 100/2) to give **7** as a white solid (71 mg, 79%), which could be further purified by crystallization in MeOH.
^{1}H NMR (300 MHz, DMSO) δ = 9.50 (s, 1 H), 8.51(s, 1 H), 8.10(dd, *J* = 6.9, 2.7 Hz, 1 H), 7.86(s, 1 H), 7.75-7.80(m, 1 H), 7.44 (t, *J* = 9.0 Hz, 1 H), 7.21 (s, 1 H), 4.95 (d, *J* = 2.4 Hz, 2 H), 3.94(s, 3H), 3.67(t, *J* = 2.4 Hz, 1 H).
^{13}C NMR (75 MHz, DMSO) δ = 156.12, 154.53, 153.21 (d, *J* = 241.2 Hz), 153.04, 147.40, 146.58, 136.73 (d, *J* = 2.1 Hz), 123.44, 122.25 (d, *J* = 6.5 Hz), 118.85 (d, *J* = 18.2 Hz), 116.57 (d, *J* = 21.5 Hz), 108.51, 107.57, 103.85, 78.85, 78.62, 56.63, 55.95;
^{19}F NMR (282 MHz, $CDCl_3$) δ = -91.81.
MS *m/z*:
LR-ESI: Calcd. for $C_{18}H_{14}ClFN_3O_2$ ($M+H^+$) 358.1, Found 358.1 ;
HR-ESI: Calcd. for $C_{18}H_{14}ClFN_3O_2$ ($M+H^+$) 358.0759 , Found 358.0752 ;
IR: $\tilde{\upsilon}$ = 1625, 1581, 1499, 1473, 1428, 1403, 1304, 1207, 1143, 1072, 1056, 1024, 994, 932, 864, 842, 793 cm^{-1};
UV/Vis: λ_{max} = 246, 329 nm

Methyl 2-((4-((3-chloro-4-fluorophenyl)amino)-7-methoxyquinazolin-6-yl)oxy)acetate (8)
To a solution of **6** (150 mg, 0.47 mmol) in DMF (4 ml) were added methyl bromoacetate (67 μL, 0.71 mmol, 1.5 equiv.) and K_2CO_3 (97 mg, 0.71 mmol, 1.5 equiv.). The mixture was stirred at room temperature and monitored by TLC. After 5 h, the mixture was poured into crushed ice and stirred vigorously for 30 min. After being filtered and washed thoroughly with water, the affording solid was dried under vacuum to give product **8** as an off-white solid (176 mg, 96 %), which could be further purified by crystallization in MeOH.
^{1}H NMR (500 MHz, $CDCl_3$-MeOH) δ = 8.37 (s, 1 H), 7.75-7.73 (m, 1 H), 7.54 (s, 1 H), 7.47-7.45 (m, 1 H), 7.04-7.01 (m, 2 H), 4.78 (s, 2 H), 3.90 (s, 3 H), 3.89 (s, 3 H).
^{13}C NMR (126 MHz, $CDCl_3$-MeOH) δ = 169.43, 157.11, 155.77, 155.23, 153.82, 153.09, 147.08 (d, *J* = 117.18 Hz), 135.42, 124.63, 122.34 (d, *J* = 6.3 Hz), 120.62 (d, *J* = 18.6 Hz), 116.34 (d, *J* = 21.8 Hz), 108.90, 106.67, 103.94, 66.06, 56.21, 52.45.

2-((4-((3-chloro-4-fluorophenyl)amino)-7-methoxyquinazolin-6-yl)oxy)acetic acid (9)
The above methyl ester compound **8** (136 mg, 0.347 mmol) was dispersed in 45 mL 0.2 M LiOH (*i*-PrOH/H_2O = 1.2/1), and the whole mixture was stirred at 23 °C in dark for overnight. The reaction was quenched by addition of diluted HOAc to pH 5 and a gel-like solid precipitated during the time. The whole mixture was further stirred vigorously for 30 min, filtered and thoroughly washed with water, *i*-PrOH and Et_2O. After being dried in air for overnight, pure compound **9** (123 mg, 94 %) was collected and was used directly for next step.
^{1}H NMR (500 MHz, DMSO) δ = 9.62 (s, br, 1 H), 8.54 (s, 1 H), 8.13-8.10 (m, 1 H), 7.82 (s, 1 H), 7.80-7.76 (m, 1 H), 7.48 (t, 1 H, *J* = 9.0 Hz), 7.25 (s, 1 H), 4.91 (s, 2 H), 3.98 (s, 3 H);
^{13}C NMR (126 MHz, $CDCl_3$-MeOH) δ = 169.58, 156.16, 154.42, 154.27, 152.87, 152.42, 147.21 (d, *J* = 32.76 Hz), 136.64, 123.94, 122.60 (d, *J* = 6.0 Hz), 118.86 (d, *J* = 18.4 Hz), 116.62 (d, *J* = 21.7 Hz), 108.51, 106.46, 102.82, 65.08, 55.95;
^{19}F NMR (282 MHz, $CDCl_3$) δ = -45.92;

HR-ESI: Calcd. For $C_{17}H_{14}ClFN_3O_4$ ($M+H^+$) 378.0657, Found 378.0651;
UV/Vis: λ_{max} = 251, 331 nm;

Tert-butyl (2-(2-(2-((4-((3-chloro-4-fluorophenyl)amino)-7-methoxyquinazolin-6-yl)oxy)acetamido)ethoxy)ethoxy)ethyl)carbamate (10)

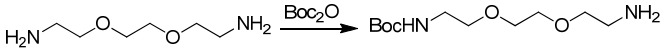

2-(2-(2-t-Butoxycarbonylaminoethoxy)ethoxy)-ethylamine: To a stirred solution of 1,8-diamino- 3,6-dioxaoctane (15.0 g, 99.6 mmol) in DCM (120 mL) was added a solution of di-t-butyl dicarbonate (10.8 g, 50.7 mmol) in Et_2O (100 mL) over 10 h. The reaction was continued with stirring for an additional 40 h during which time the whole mixture became turbid with a white solid separated. The solvent was evaporated under reduced pressure to yield crude yellow oil. This oil was subjected to separation by flash column chromatography on silica gel (prepared with 1% Et_3N in DCM) using DCM/MeOH (19:1–10:1) as eluent to yield the product 5.9 g (46.9 %). as clear oil with a little yellow color. This material was directly used in the next step.

^{1}H-NMR (300 MHz, $CDCl_3$, 23 ºC) δ = 5.15 (br s, 1 H), 3.58 (s, 4 H), 3.49 (m, 4 H), 3.25 (q, 2 H, *J* = 5.2 Hz), 2.83 (t, 2 H, *J* = 5.2 Hz), 1.60 (br, s, 2 H), 1.40 (s, 9 H).

To a stirred solution of **9** (38 mg, 0.101 mmol) in anhydrous DMF (2.0 mL) was added O-(benzotriazol-1-yl)-N,N,N',N'-tetramethyluronium hexafluorophosphate (HBTU, 49 mg, 0.13 mmol, 1.3 equiv.) followed by the addition of DIPEA (0.056 mL, 0.32 mmol, 3.2 equiv.). The resulting mixture was stirred in black at 23 °C for 1 hr and then 2-(2-(2-t-Butoxycarbonylaminoethoxy)ethoxy)-ethylamine (32 mg, 0.13 mmol, 1.3 equiv.) in anhydrous DMF (0.5 mL) was added in dropwise. The reaction was kept stirred for 20 h under Ar. When the reaction was complete, monitored by TLC (SiO_2), most of the solvent was evaporated and the residue was taken up with DCM. The organic phase was washed with water (2 x), Sat. aq. $NaHCO_3$ (1 x) and brine. After being dried over Na_2SO_4, the solvent was concentrated under vacuum and the residue was purified by flash chromatography (SiO_2, Eluent: DCM/MeOH = 100/0.5 to 100/2) to afford the product **10** (60 mg, 99 %).

^{1}H NMR (300 MHz, $CDCl_3$) δ = 8.58 (s, 1 H), 7.85-7.93 (m, 1 H), 7.69 (s, 1 H), 7.55-7.62 (m, 1 H), 7.37 (s, br, 1 H), 7.17 (s, 1 H), 7.09 (t, *J* = 9.0 Hz, 1 H), 5.14 (s, br, 1 H), 4.71 (s, 2 H), 3.93 (s, 3 H), 3.55 (s, br, 4 H), 3.42-3.55 (m, 6 H), 3.18-3.32 (m, 2 H), 1.38 (s, 9 H);

^{13}C NMR (75 MHz, $CDCl_3$) δ = 168.60, 157.14, 156.36, 155.09, 154.87 (d, *J* = 244.5 Hz), 153.57, 153.44, 153.24, 147.15, 135.65, 124.82, 122.60 (d, *J* = 6.4 Hz), 120.68 (d, *J* = 18.4 Hz), 116.45 (d, *J* = 21.9 Hz), 109.02, 107.39, 104.94, 79.63, 70.33, 70.21, 69.57, 68.81, 56.33, 55.23, 40.47, 39.03, 28.53;

HR-ESI: Calcd. For $C_{28}H_{36}ClFN_5O_7$ ($M+H^+$) 608.2288, Found 608.2276;

IR: $\tilde{\upsilon}$ = 3412, 3332, 2977, 2931, 2876, 1674, 1627, 1580, 1531, 1501, 1472, 1429, 1393, 1366, 1248, 1217, 1169, 1141, 1103, 1074, 1001, 930, 909, 846, 794 cm^{-1};

UV/Vis: λ_{max} = 247, 330 nm.

Ethyl 2-(4-(3-((4-((3-chloro-4-fluorophenyl)amino)-7-methoxyquinazolin-6-yl)oxy)propyl)piperazin-1-yl)acetate (11)

Ethyl 2-(4-(3-chloropropyl)piperazin-1-yl)acetate: To a solution of commercially available ethyl 2-(piperazin-1-yl)acetate hydrochloride (1 g, 5.81 mmol) in ACN (35 mL) was added 1-bromo-3-chloropropane (0.69 mL, 6.97 mmol, 1.2 equiv.). And Et_3N (3.26 mL, 23.2 mmol, 4 equiv.) was dropped into the above mixture at room temperature slowly. The reaction was stirred at room temperature and monitored by TLC. 24 hrs later, the mixture was filtered and washed with excess ACN. The filtrate was combined, evaporated to dry and the resulting crude material was further purified by flash chromatograph with DCM/MeOH = 9/1 as eluent to afford the pure product **10** (464 mg, 32 %). ***Note: the starting material, commercially available ethyl 2-(piperazin-1-yl)acetate hydrochloride, is a mixture which might account for the low yield.***

^{1}H NMR (300 MHz, $CDCl_3$) δ = 4.14 (q, 2 H, *J* = 7.2 Hz), 3.55 (t, 2 H, *J* = 6.6 Hz), 3.17 (s, 2 H), 2.40-2.69 (m, 10 H), 1.88-1.97 (m, 2 H), 1.23 (t, 3 H, *J* = 7.2 Hz);

^{13}C NMR (75 MHz, $CDCl_3$) δ = 170.35, 60.76, 59.56, 55.47, 53.01, 43.27, 29.83, 14.38.

Method A: To a solution of **6** (130 mg, 0.41 mmol) in DMF (3 ml) were successively added K_2CO_3 (112 mg, 0.81 mmol, 2.0 equiv.), ethyl 2-(4-(3-chloropropyl)piperazin-1-yl)acetate (**I-10** 202 mg, 0.81 mmol, 2.0 equiv.), NaI (183 mg, 1.22 mmol, 3.0 equiv.). The whole mixture was warmed to 60°C for reaction and monitored by TLC. 10 hour later, TLC showed most of the starting material disappeared and the reaction was quenched by being poured into well stirred ice water. After being extracted with DCM (3 X 30 mL), washed with water and brine, the organic phase was dried over Na_2SO_4 and evaporated to dry. The resulting crude material was further purified by flash chromatograph with DCM/MeOH = 9/1 as eluent to afford the pure product **I-11** (123 mg, 56 %) as a semi-solid.

^{1}H NMR (300 MHz, $CDCl_3$) δ = 8.74 (s, 1 H), 8.66 (s, 1 H), 7.89 (dd, 1 H, *J* = 6.3, 2.4 Hz), 7.55-7.60 (m, 1 H), 7.45 (s, 1 H), 7.16 (s, 1 H), 7.08 (t, *J* = 8.7 Hz, 1 H), 4.17 (q, 2 H, *J* = 6.9 Hz), 3.98 (t, 2 H, *J* = 6.6 Hz), 3.87 (s, 3 H), 3.18 (s, 2 H), 2.40-2.69 (m, 10 H), 1.93-2.00 (m, 2 H), 1.27 (t, 3 H, *J* = 6.9 Hz);

^{13}C NMR (75 MHz, $CDCl_3$) δ = 170.56, 156.70, 155.18, 154.63 (d, *J* = 247.83 Hz), 153.46, 148.92, 147.31, 135.71, 124.31, 121.97 (d, *J* = 6.2 Hz), 120.81 (d, *J* = 18.4 Hz), 116.48 (d, *J* = 21.7 Hz), 109.32, 107.38, 101.84, 67.64, 60.83, 59.30, 56.17, 54.77, 52.82, 52.72, 26.08, 14.31.

^{19}F NMR (282 MHz, $CDCl_3$) δ = -94.94.

LR-ESI: Calcd. For $C_{26}H_{32}ClFN_5O_4$ ($M+H^+$) 532.2, Found 532.2;

HR-ESI: Calcd. for $C_{26}H_{32}ClFN_5O_4$ ($M+H^+$) 532.2127, Found 532.2128;

IR: $\tilde{\upsilon}$ = 3289, 2940, 2821, 1743, 1624, 1579, 1526, 1500, 1472, 1428, 1397, 1354, 1337, 1216, 1172, 1141, 1069, 1032, 1011, 931, 858, 821, 794 cm^{-1};

UV/Vis: λ_{max} = 246, 331 nm;

Method B: To a solution of **I-6** (390 mg, 1.22mmol) in DMF (9 ml) were successively added K_2CO_3 (338 mg, 2.45 mmol, 2.0 equiv.), ethyl 2-(4-(3-chloropropyl)piperazin-1-yl)acetate (**I-10**, 606 mg, 2.45 mmol, 2.0 equiv.), NaI (549 mg, 3.66 mmol, 3.0 equiv.). The whole mixture was warmed to 60°C for reaction and monitored by TLC. 40 hour later, TLC showed most of the starting material disappeared and the reaction was quenched by being poured into well stirred ice water. After being extracted with DCM (3 x 30 mL), washed with water and brine, the organic phase was dried over Na_2SO_4 and evaporated to dry. The resulting crude material was further purified by flash chromatograph with DCM/MeOH = 9/1 as eluent to afford the pure product **I-11** (600 mg, 92 %) as a semi-solid. The data are the same as reported above.

2-(4-(3-((4-((3-chloro-4-fluorophenyl)amino)-7-methoxyquinazolin-6-yl)oxy)propyl)piperazin-1-yl)acetic acid (12)

The ethyl ester compound **11** (290 mg, 0.545 mmol) was dispersed in 45 mL 0.2 M LiOH (*i*-PrOH/H_2O = 1.2/1), and the whole mixture was stirred at 23 °C in the absence of direct light. The reaction was monitored by TLC over 6 h until all the starting material was transformed to the product. The *i*-PrOH was evaporated under vacuum until a pale-while solid precipitate was formed. The residue was diluted with water and 1 N acetic acid was added dropwise to adjust pH to 5 which resulted in additional pale-while solid precipitate formation. The solid was filtered, washed with water, *i*-PrOH and Et_2O successively. The solid was further dried under vacuum to afford the product **12** (165 mg, 60 %). The filtrate was evaporated under vacuum to remove the organic solvent and a little more pale-white solid precipitated.

Solubility Test

solvent	DCM	MeOH	i-PrOH	DCM-MeOH	DMF	DMSO
r.t.	×	×	×	√	√	√
Δ	×	√	√	N/A	N/A	N/A
Sonication	×	√	N/A	N/A	N/A	N/A

Note: the product could be dissolved in i-PrOH, so it might not be a good choice to use i-PrOH in the above washing steps.

^{1}H NMR (300 MHz, DMSO-*d6*) δ = 9.62 (br, s, 1 H), 8.50 (s, 1 H), 8.13 (dd, 1 H, *J* = 6.9, 2.5 Hz), 7.78-7.83 (m, 2 H), 7.44 (t, *J* = 9.0 Hz, 1 H), 7.19 (s, 1 H), 4.17 (t, 2 H, *J* = 6.0 Hz), 3.94 (s, 3 H), 3.18 (s, 2 H), 2.64-2.84 (m, 4 H), 2.40-2.60 (m, 6 H), 1.92-2.07 (m, 2 H);
^{13}C NMR (75 MHz, DMSO-*d6*) δ = 169.82, 156.04, 154.49, 153.15 (d, *J* = 241.5 Hz), 152.63, 148.34, 146.98, 136.89, 123.50, 122.35 (d, *J* = 6.75 Hz), 118.78 (d, *J* = 17.85 Hz), 116.52 (d, *J* = 21.45 Hz), 108.82, 107.28, 102.53, 67.09, 58.73, 55.89, 54.28, 51.87, 51.78, 26.14.
^{19}F NMR (282 MHz, $CDCl_3$) δ = -120.13.
LR-MALDI: Calcd. for $C_{24}H_{28}ClFN_5O_4$ ($M+H^+$) 504.2, Found 503.7;
HR-ESI: Calcd. for $C_{24}H_{28}ClFN_5O_4$ ($M+H^+$) 504.1814, Found 504.1800;
IR: $\tilde{\upsilon}$ = 3368, 2952, 2838, 1625, 1581, 1500, 1473, 1429, 1400, 1247, 1234, 1218, 1144, 1004, 855 cm^{-1};
UV/Vis: λ_{max} = 249, 331 nm;

Appendix 5: Cell Uptake and Growth Phenotype Studies with Peptides, Peptoids, and Conjugates

Confocal Imaging: MDA-MB-231 cells were exposed to fluorescently tagged 'cell-penetrating' peptoids, the TAT peptide nuclear localization sequence (NLS), or simply 5-carboxyfluorescein (listed as "no compound") at equivalent dosage concentrations. Increased levels of cellular uptake were observed when fluorescein was coupled to the TAT peptide or NLys peptoids. Furthermore, cellular uptake was dependent on the length of the NLys peptoid conjugate, as extending the length of the peptoid from seven to nine residues significantly enhanced the effect.

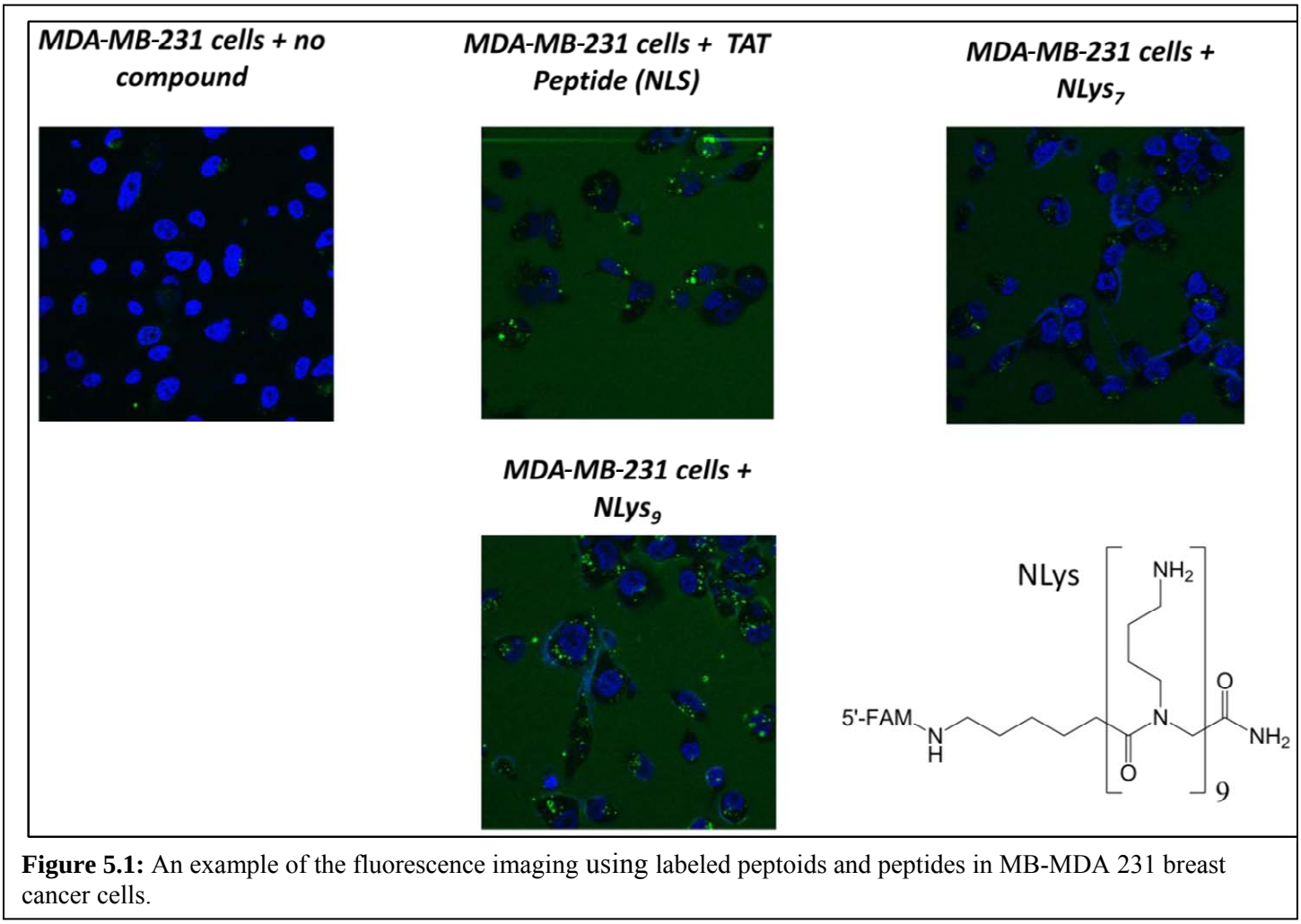

Figure 5.1: An example of the fluorescence imaging using labeled peptoids and peptides in MB-MDA 231 breast cancer cells.

Growth Phenotype of Molecular Entities with Breast Tumor Cell Lines

Cell lines and cell culture: Human breast cancer panel cell lines were obtained from the American Type Culture collection and were initially cultivated in Dulbecco's modified Eagle's medium (DMEM) containing 10% fetal bovine serum (FBS) were cultured at 37 C in a humidified atmosphere at 5 % CO_2 and 95% air. Cells for assay were cultivated in Dulbecco's Modified Eagle's Medium was low glucose (1000 mg/L glucose) with L-glutamine, without phenol red, powder (D2902 Sigma) buffering was achieved using sodium bicarbonate.

Cell viability by MTT assay: Potential growth inhibitory activity of the test compound was determined by MTT assay. Actively growing cells were detached using TypLE select (Life Technologies). Each cell line was seeded on 96-well microplates at a density of 1.0×10^4cells/well in 80 uL and allowed to attach to the tissue culture treated plastics after placing the 96 well plate in a Nunc overplate for evaporation control for 4 hours. A five-step, two-fold drug dose dilution series was prepared robotically in a Biomek 3000 (Beckman Coulter) in medium described previously. The test compounds were delivered as 20 uL aliquots mixed into 80 uL cell aliquot for final exposure concentrations. Exposure to compound for 4 days occurred to allow for the slow growth of certain breast cell lines.

A Day 0 plate for each cell line was developed by the robotic addition of 10 uL of 5 mg/ml MTT (in DMEM low glucose 0% FBS and without phenol red) per well and allowed to develop for 4 hours after being placed in a Nunc overplate to control evaporation. Then 100 uL of MTT solvent (0.1 N HCl in anhydrous

isopropanol with 10% Triton X-100) was added, the assay plates were tightly wrapped in foil and placed in sealed zip lock bags to allow the solubilization of the MTT formzan product to occur and progress to solubilization for reading in a spectrophotometer at 570 nm. Subtraction of background absorbance measured at 690 nm was not performed. Day 4 test plates were developed as described above. Cell growth values were plotted using an Excel spreadsheet as described previously (Woods et al., 2011) and then graphed using GraphPad Prism (Version 5.02, GraphPad software).

Reference: Woods, J. R., Mo, H., Bieberich, A. A., Alavanja, T., & Colby, D. A. (**2011**). Fluorinated Amino-Derivatives of the Sesquiterpene Lactone, Parthenolide, as ^{19}F NMR Probes in Deuterium-Free Environments. *Journal of Medicinal Chemistry*, **54**, 7934-7941.

Figure 5.2

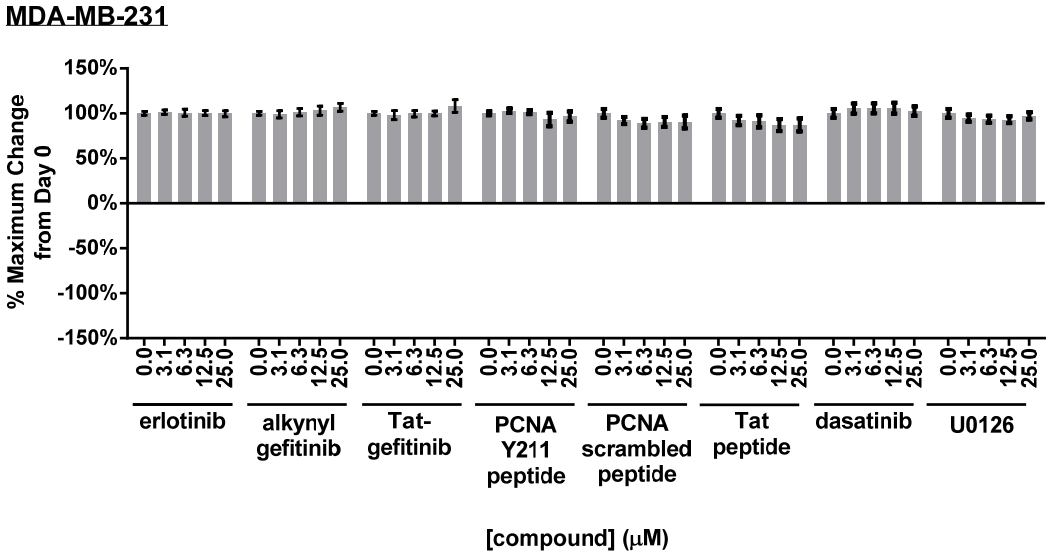

A.

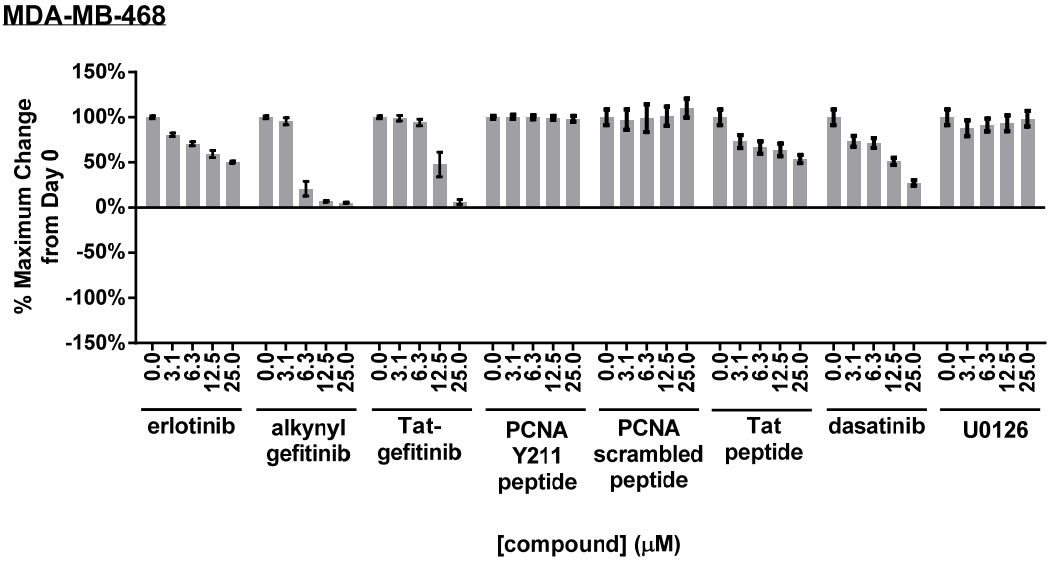

B.

HCC1567

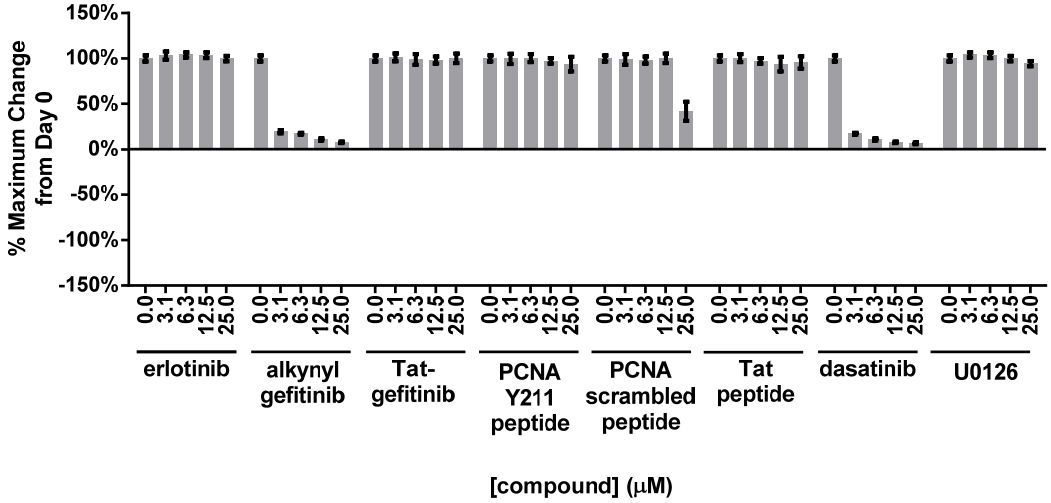

C.

MCF7

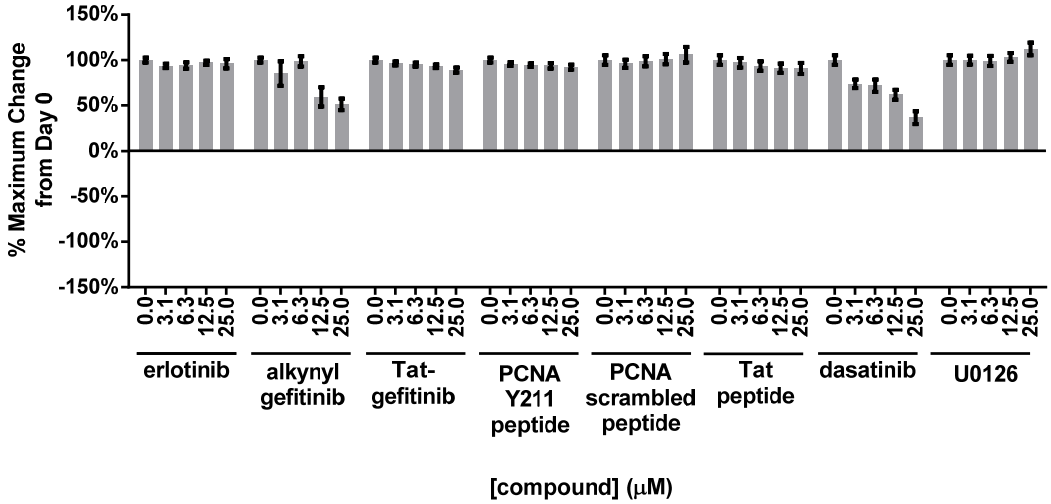

D.

T47D

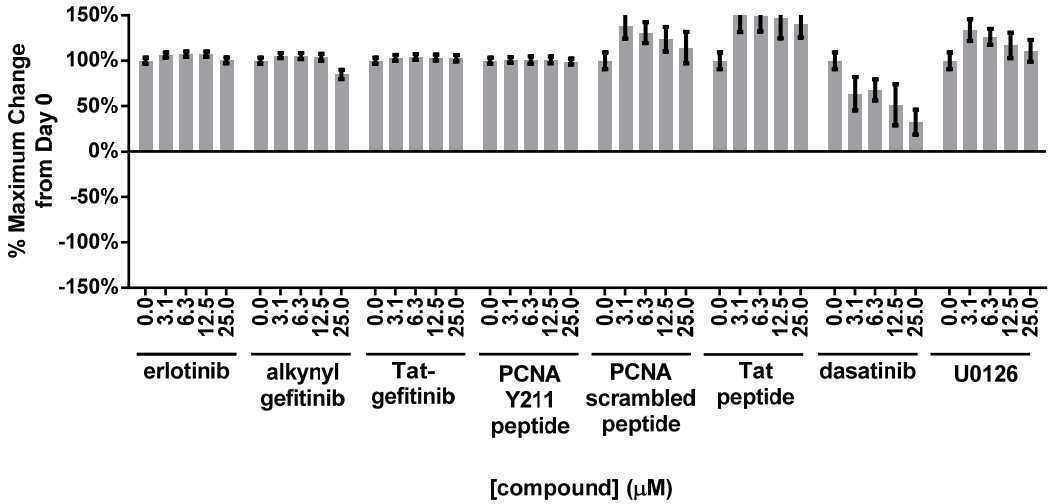

E.

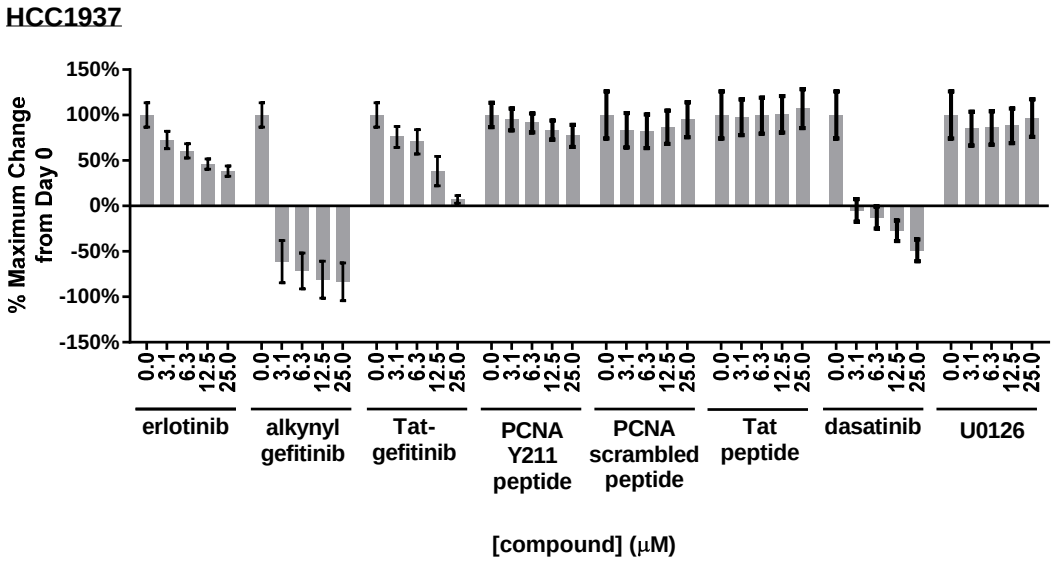

F.

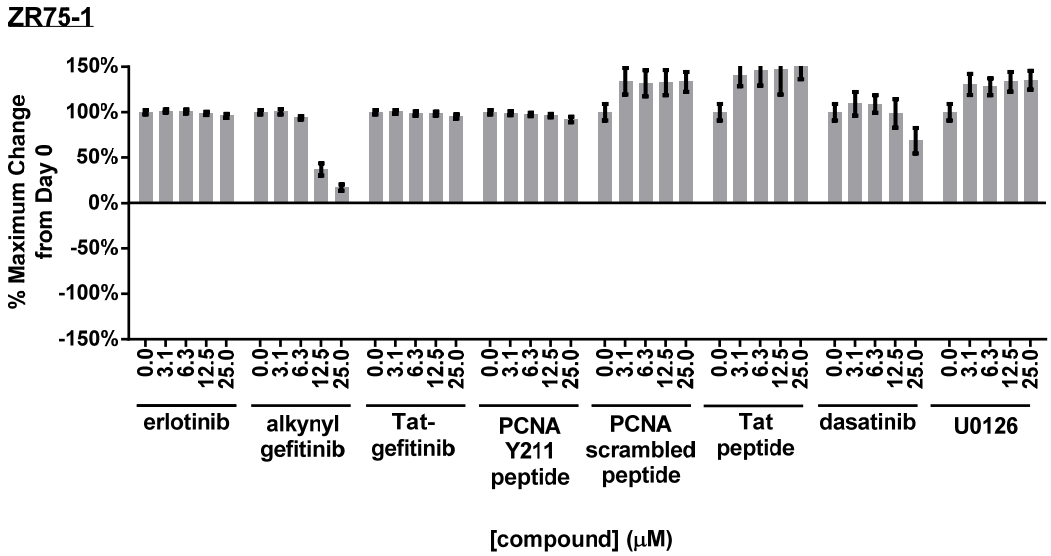

G.
H.

Appendix 6. Cellular Fractionation and Analysis of Nuclear PCNA Isoforms

Nuclei Isolation and Fractionation (Aims 1b and 2b)
To investigate differences in chromatin-unbound and -bound nuclear fractions, a method for nuclei isolation and fractionation was developed. The method of nuclei isolation requires the use of a sucrose gradient and Dounce homogenization. Fractionation of nuclei is performed using differences in detergent properties. A non-ionic detergent (Triton) was effective at removing any non- or loosely-bound chromatin associated proteins, whereas, a stronger ionic detergent (SDS) was capable of removing proteins that are chromatin-bound. Both Aims 1b and 2b both require the use of nuclear fractionation to test the basic hypothesis that PCNA phosphorylation regulates PCNA stability onto chromatin. Enhanced stability of PCNA translates to an increase in PCNA function as a cancer-specific regulator of DNA repair and checkpoint. Demonstration of nuclear fractionation will be integrated into key experiments proposed to answer the specific research questions.

Development and Optimization of a Protein Isoform Profiling System (Aim 2b),
To identify changes of PCNA isoforms, a protein isoform profiling system has been developed. This platform is capable of fractionating and enriching for PCNA isoforms using free flow electrophoresis (FFE). FFE is a high-

throughput technique that fractionates cellular lysate based on isoelectric point. Each of the 96 fractions was analyzed using a reverse-phase immunological assay. Detection of the reverse-phase immunological assay has been focused on fluorescence but will be shifted to SERRS as soon as all steps are further optimized.

Method development focused on PCNA isoform enrichment by optimizing the separation gradient. The final method utilizes a denatured, pH 3-10 pH gradient. This gradient enhances stability and allows for better resolution of PCNA isoforms (<0.1 pH unit between fractions in linear pH range). In addition, various additives were added to the separation buffers to stabilize the gradient from changes due to sample application.

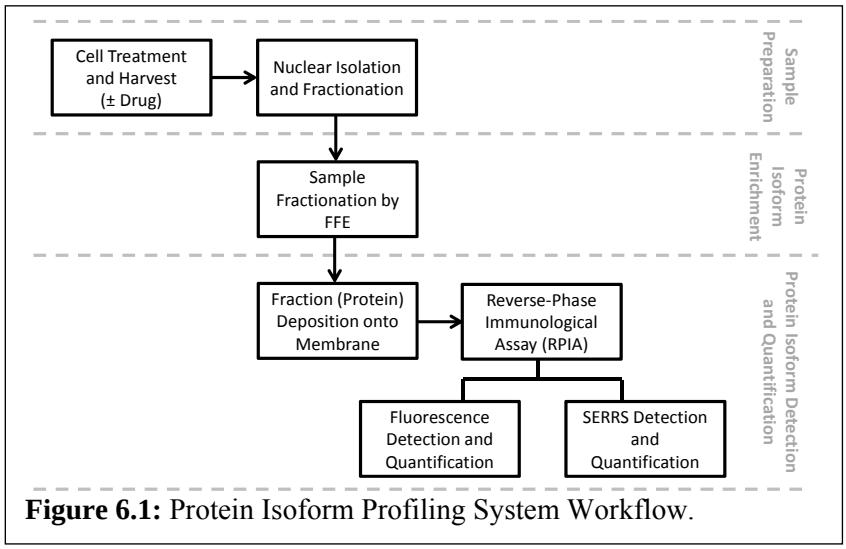

Figure 6.1: Protein Isoform Profiling System Workflow.

The major issue with the current separation gradient is the potential for protein precipitation at high concentrations of protein. When sample concentrations greater than 5 mg/mL were loaded into the separation chamber, the protein visually precipitated under denatured conditions causing shifts in the pH gradient. This resulted in poor resolution of the PCNA isoforms.

In addition, fractionating samples by FFE dilutes out the sample to the point where analysis becomes very difficult. A significant amount of time was devoted to enhancing sample detection by utilizing a variety of sample deposition and detection strategies. The best strategy currently relies on concentrating the protein through the preparation of a dot blot followed by performing a reverse-phase immunological assay (RPIA).

Detection strategies for the RPIA have been focused on use of fluorescence readout. The fluorescence readout has allowed for faster turnaround during the isoform optimization process. More in-depth analysis was performed to look at shifts in PCNA isoform populations between runs. PCNA isoform populations were determined based on pH gradient value, and an enzyme-linked immunosorbent assay (ELISA) was developed to validate the presence of PCNA in these fractions. The ELISA assay has also been adapted to investigate the phosphorylation status of PCNA. Figure 2 shows a separation of PCNA isoform separation of MCF7 breast cancer cells using fluorescence detection.

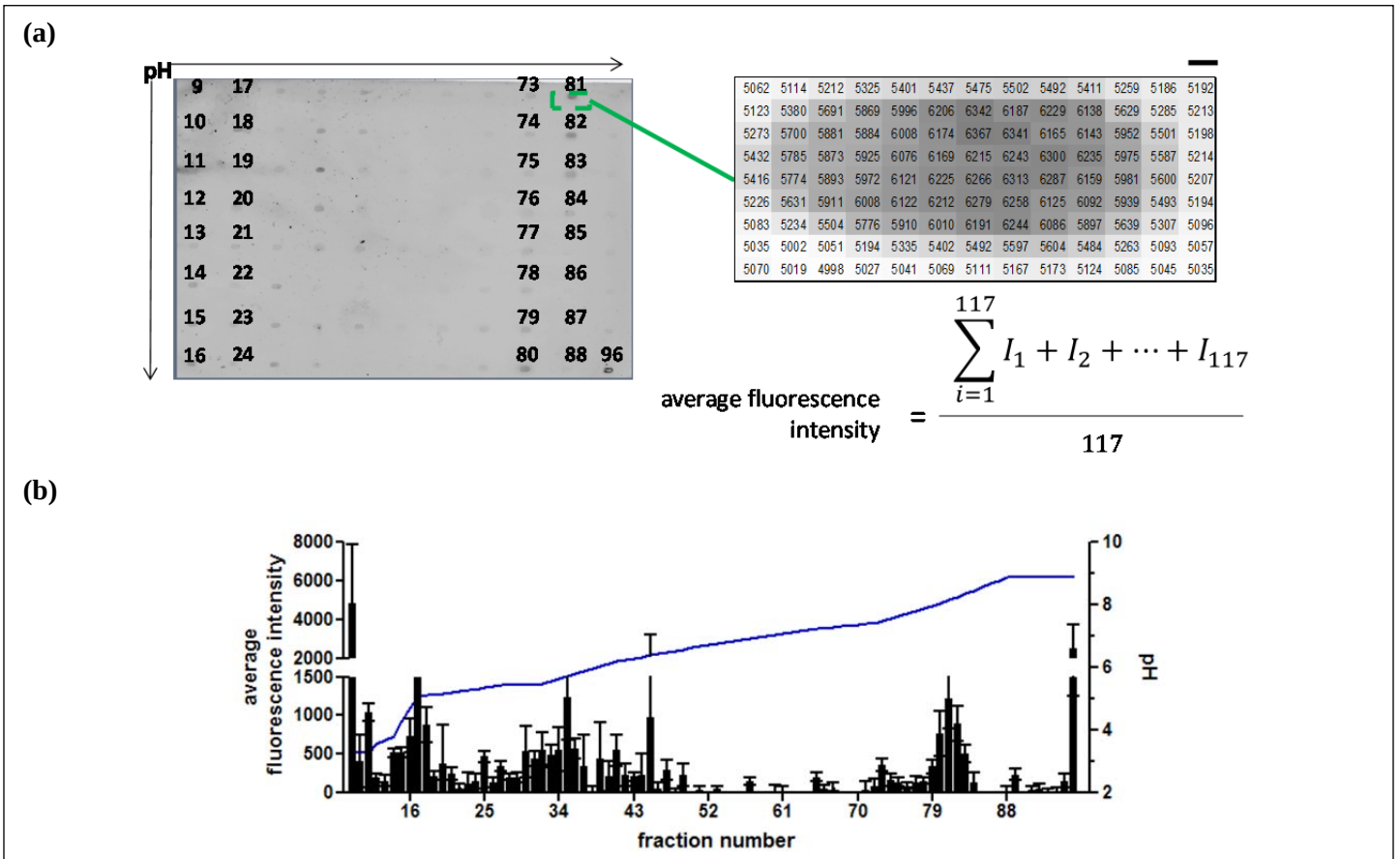

Figure 6.2. PCNA Isoform Separation as Determined by Reverse-Phase Immunological Assay. Chromatin-bound MCF7 breast cancer cell nuclear lysate was fractionated by free flow electrophoresis and the fractions were dot blotted onto a piece of PVDF membrane. A reverse-phase immunological assay was performed using a PC10 monoclonal total PCNA antibody and a fluorescently-labeled secondary antibody reporter. **(a)** Membrane was imaged using a Typhoon Trio+ image scanner using an excitation of 488nm and an emission of 526nm. Individual pixel intensities from each spot of protein deposition were averaged. **(b)** The average intensity of each spot deposition versus fraction number and pH. These demonstrate four different populations of PCNA isoforms.

The ultimate goal of this platform is to be able to quantify the levels of the various PCNA isoforms using surface-enhanced Resonance Raman spectroscopy (SERRS). Our laboratory has thoroughly characterized the properties of isotopically-labeled rhodamine-6G (R6G) fluorescent dyes for multiplex SERRS detection. The technology developed was transferred to these blots to accurately quantify the presence of various modifications on PCNA. To achieve this task, antibodies were labeled with the d_0 and d_4 encoded rhodamine-6G. Process optimization was performed for more efficient synthesis of these fluorescent dyes and antibody labeling. Scheme 1 shows the improved synthesis of d_0 and d_4-R6G for antibody labeling. The labeling efficiencies of each of these dyes were determined to be equivalent (Table 1).

A PCNA probed blot with d_0-R6G-labeled PC10 monoclonal PCNA antibody was silver and gold stained using an in-house method and Raman signals due to the fluorophore were collected. Figure 3 shows the Raman spectra collected from various fractions on PVDF membrane. This method has been shown to work well with the optimized isoform separation platform. However, further optimization is still needed to determine optimal protein deposition onto PVDF.

Scheme 6.1. Synthesis of R6G-Labeling Reagent

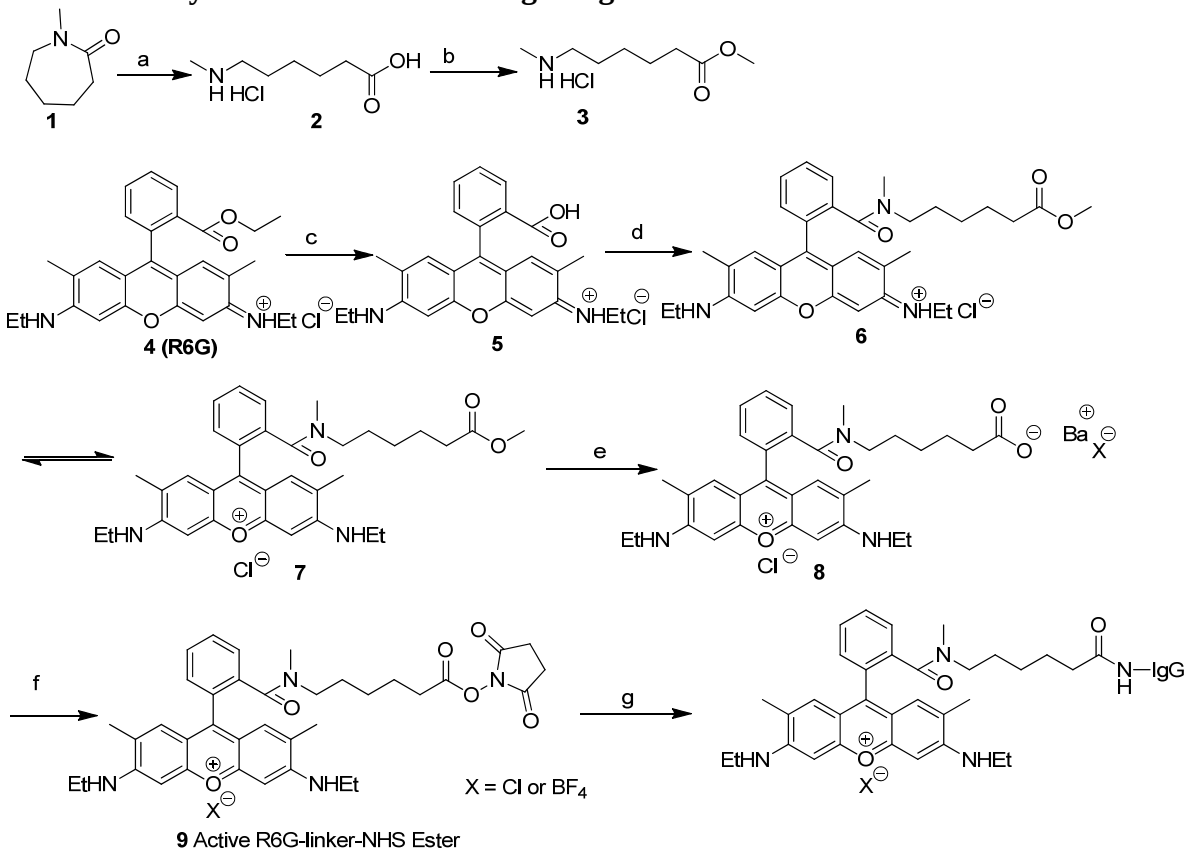

Conditions:
a): HCl (conc. aq.), reflux 5 d; b): HCl (g), MeOH, rt, overnight, quantitative for 2 steps; c): NaOH (aq. 1N), reflux 8 hr, quantitative; d): **3** (1.2 eq.), HBTU (1.2 eq.),DIPEA (4.5 eq.), DMF, rt, 6 - 8 hr 92 %; e): $Ba(OH)_2{\cdot}H_2O$ (1.2 eq.), $MeOH/H_2O$ = 2/1, rt, 18 hr; f): TSTU (1.5 eq.), ACN, rt, 5~6 hr, quantitative; g): IgG (1:100 stoichometric ratio), $NaCO_3$, pH 8.0, rt, dark, 20 min.

Table 6.1: Labeling Efficiencies of d_0 and d_4-R6G Labeled IgG

sample	A_{280}	A_{530}	Labeling Efficiency (A_{530}/A_{280})×100%	
d_0-R6G-IgG 1:100, replicate 1	0.3436	0.2592	75.4%	
d_0-R6G-IgG 1:100, replicate 2	0.3512	0.2620	74.6%	
d_0-R6G-IgG 1:100, replicate 3	0.3424	0.2484	72.5%	74.2 ± 1.5%
d_4-R6G-IgG 1:100, replicate 1	0.2304	0.1683	73.0%	
d_4-R6G-IgG 1:100, replicate 2	0.2705	0.1810	66.9%	
d_4-R6G-IgG 1:100, replicate 3	0.2676	0.1837	68.6%	69.5 ± 3.2%

(a)

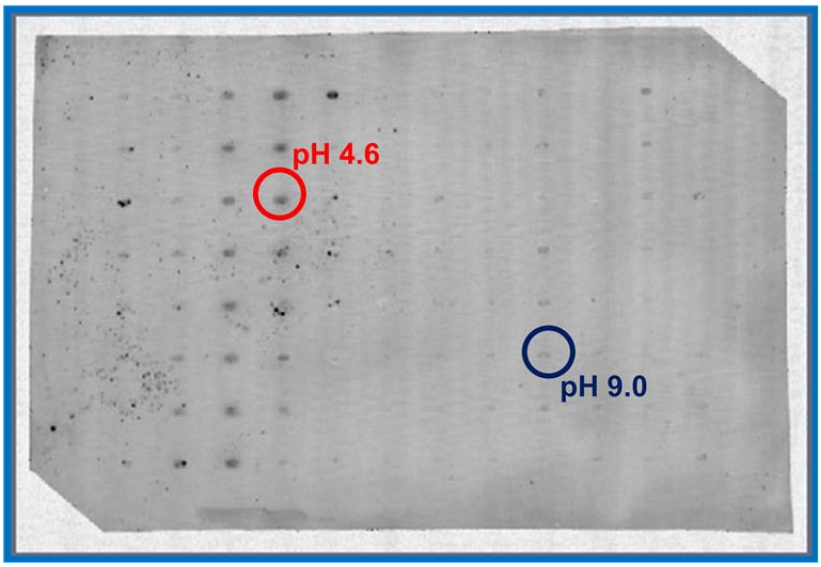

(b)

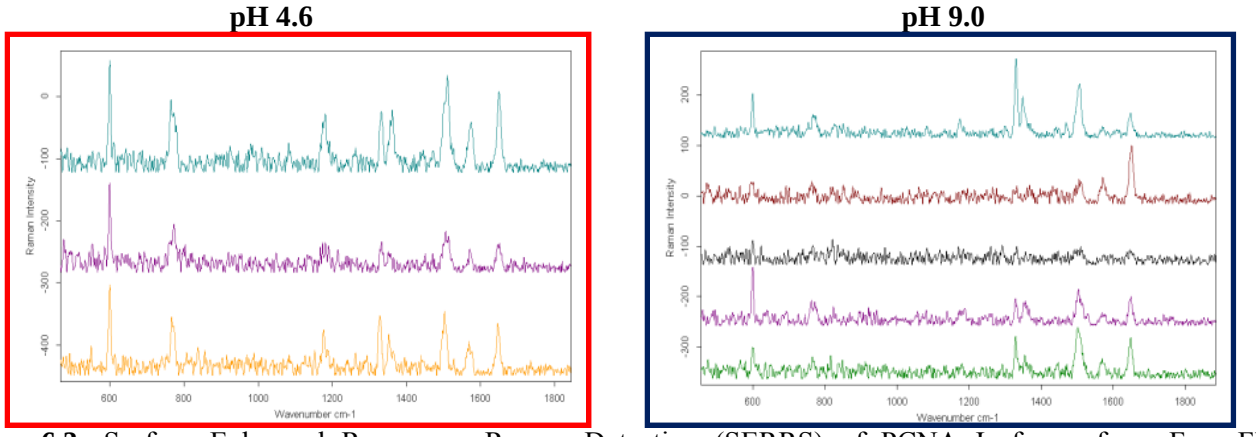

Figure 6.3: Surface Enhanced Resonance Raman Detection (SERRS) of PCNA Isoforms from Free Flow Electrophoresis Fractions. Nuclear chromatin-bound MCF-7 protein lysate was separated by free flow electrophoresis over a pH gradient of 3-10. A dot blot of each fraction was performed on PVDF membrane and probed for presence of total PCNA with PC10 monoclonal PCNA antibody followed by *d6*-R6G-labeled anti-mouse IgG. SERRS detection was performed on each of the spots to indicate presence of PCNA. Dot blot shows protein levels 50-fold greater amount.